Heterogeneous Polar Amplification *

María Dolores Gadea Rivas †
University of Zaragoza

Jesús Gonzalo ‡
U. Carlos III de Madrid

April 24, 2025

Abstract

Arctic and Antarctic climate evolution is crucial for understanding global climate dynamics. This study grounds in the framework of Gadea and Gonzalo (2020, 2025) to analyze different distributional characteristics (beyond the average) of polar temperature measurement as time series objects, enabling the definition and robust testing of polar warming, its acceleration, and amplification. Our findings provide a quantitative description of the warming processes affecting the polar regions. The research examines measurements of temperature in the Arctic (1900-2019) and the Antarctic (1960-2022). Key findings include: (i) Clear Arctic warming since 1900 across all quantiles, with more pronounced warming in lower quantiles since 1950. No significant warming was observed in Antarctica in all of the temperature quantiles; (ii) Arctic warming acceleration since 1960, particularly in lower and middle quantiles, with no apparent peak reached yet; (iii) Consistent Arctic amplification is slightly below 2 and stable across analyzed periods. Lower quantiles (corresponding with winter in the higher latitudes) show larger amplification than the mean. Since 1960, amplification has extended to upper quantiles, except the 90th and 95th percentiles; (iv) Analysis of the internal Arctic amplification shows that this is primarily a lower-quantile phenomenon, Arctic amplification is stronger in higher latitude winters and this affects the speed at which the ice in the Arctic is disappearing.

The study's amplification estimates are lower than some observational studies but align more closely with climate model projections. The paper concludes by comparing these results to the equivalent global temperature trends.

JEL classification: C31, C32, Q54
Keywords: Climate change; Global-Local warming; Distributional characteristics; Trends; Quantiles; Temperature distributions; Polar Warming; Polar Acceleration; Polar Amplification.

*We are very grateful to an editor, two anonymous referees and conference and seminar participants to seminar participants at 11th CFE-2017 London, 2nd Conference on Econometric Models of Climate Change, Oxford-2017, IAAE-2019, Cyprus and to Phil Jones, David Lister and Igor Polyakov for his valuable help in collecting and interpreting the data. The financial support from: Gobierno de Aragón and European Regional Development Fund (ERDF, EU) funds under grant, LMP71-18; Spanish Ministerio de Ciencia e Innovación, Agencia Española de Investigación MCIN/AEI /10.13039/501100011033 and European Regional Development Fund (ERDF, EU) under grants PID2020-114646RB-C44, PID2023-147593NB-I00 and CEX2021-001181 ((María de Maeztu); Spanish Ministerio de Ciencia e Innovación, Agencia Estatal de Investigación MCIN/AEI /10.13039/501100011033 and Unión Europea NextGenerationEU/PRTR, under grant with reference TED2021-129784B-I00.; Comunidad de Madrid under grands grants EPUC3M11 and V PRICIT), is gratefully acknowledged.

† Department of Applied Economics, University of Zaragoza. Gran Vía, 4, 50005 Zaragoza (Spain). Tel: +34 9767 61842, fax: +34 976 761840 and e-mail: lgadea@unizar.es

‡ Department of Economics, University Carlos III, Madrid 126 28903 Getafe (Spain). Tel: +34 91 6249853, fax: +34 91 6249329 and e-mail: jesus.gonzalo@uc3m.es

1 Introduction

The Intergovernmental Panel on Climate Change (IPCC, 2022) emphasized the importance of stating of Climate in the Polar regions: "*Polar regions (Figure CCP6.1) are considered flagship areas for climate change, since some of the most extreme climate change impacts that are projected to occur by 2050 elsewhere in the world have already been observed in the Arctic and Antarctic and have resulted in transformative and unprecedented change. Polar regions are not only home to cultural keystone species such as polar bears (Arctic) and penguins (Antarctic) but they also play fundamental roles in regulating the global climate system and in the provision of ecosystem service for the global community...*" The same report highlights the significant changes occurring in polar regions, particularly the Arctic: "*Climate change impacts and cascading impacts in polar regions, particularly the Arctic, are already occurring at a magnitude and pace unprecedented in recent history (very high confidence), and much faster than projected for other world regions (high confidence1).*" Both statements reflect the critical role polar climate behavior plays in global climate change, given the Arctic's interactions with the global climate system. The phenomenon of polar amplification—where warming is disproportionately concentrated at high latitudes—suggests that temperature increases in the Arctic are more pronounced than in the rest of the Northern Hemisphere. While initially attributed to the albedo feedback mechanism, polar amplification is now understood as a complex process with distinct nuances in each polar region.[1]

A substantial body of literature addresses trends in polar temperatures and the amplification effect. As it is well-know, this effect is due to Ice-Albedo Feedback, Lapse Rate Feedback, Cloud Feedbacks, Oceanic Heat Transport and Increased Water Vapor. Prominent studies include those by Tuomenvirta et al. (2000), Comiso (2003), Polyakov et al. (2003), McBean et al. (2005), Steele et al. (2008), Bekryaev et al. (2010), Yamanouchi (2011), Miller et al. (2010), Serreze (2011), Wang et al. (2012), Singh (2013), Comiso and Hall (2014), and Matthes et al. (2015). Research specifically focused on polar amplification is extensive, with notable contributions from Langen and Alexeev (2007), Francis and Vavrus (2012), Screen (2013), Cohen et al. (2018, 2019), IPCC6 (2021), Constable et al. (2022), Rantanen et al. (2022), Liu et al. (2024) and Zhou et al. (2024). Studies exploring its causes and mech-

[1] For a review of the different causes of the amplification phenomenon, see Cohen et al. (2019) and Rantanen et al. (2022).

anisms include Johannessen et al. (2016), Cohen et al. (2019), and Previdi et al. (2021). Recently, Brock and Miller (2024) have sought to integrate elements of climate science into economic and econometric models that address this phenomenon. Other research suggests that the sensitivity of sea ice to seasonal temperature variability implies that a clearer understanding of distributional temperature trends is essential for improving sea-ice forecasting and modeling (e.g., Hueze and Jahn, 2024).

Two common conclusions emerge from these studies. Climate change in the Arctic manifests with the strongest warming trends globally, albeit with nuances. Methodologically, most studies focus on average temperature trends, often neglecting distributional aspects that could provide additional insights. The range of values for Arctic Amplification (AA) goes from 1.5 to 4. Our contribution builds on this foundation by extending the analysis beyond average temperature trends to include distributional characteristics such as moments and quantiles. Following the framework of Gadea and Gonzalo (2020, hereafter GG2020) and Gadea and Gonzalo (2025, hereafter GG2025), we model polar temperatures as a functional stochastic process, extracting distributional characteristics as time series objects.

From a methodological point of view, this work complements recent climate studies that go beyond average temperatures to analyze the evolution of entire temperature distributions. For instance, Donat et al. (2012) investigate shifts in the temperature probability density, while Reich (2012) applies quantile trend regression to detect differential slopes across quantiles. However, these approaches face limitations: Donat et al.'s method requires long stationary periods, which can be problematic with non-stationary temperature data, while Reich focuses on the mean temperature process rather than the full unconditional temperature distribution. Chapman et al. (2023) treat climate as a dynamic distribution, evaluating relative changes across quantiles and geographical locations. Nevertheless, their graphical approach lacks statistical testing for trend trajectories. Ji et al. (2014) employ multidimensional ensemble empirical mode decomposition (MEEMD) to extract residual trends and detect warming patterns. However, MEEMD does not easily enable statistical comparisons of entire temperature distributions or the determination of specific warming types within regions. Our methodology overcomes these challenges by transforming distributional characteristics into time series objects. This allows us to test important climate hypothesis and handle with many types of non-stationarity situations.

More specifically, this paper presents a robust quantitative methodology, grounded in the frameworks of GG2020 and GG2025, to rigorously assess the presence, acceleration, and amplification of warming in the Polar regions. In contrast to much of the conventional climate literature, which tends to emphasize changes in average temperatures, this approach examines the full distribution of temperature values. By shifting the focus from mean trends to distributional dynamics, this study offers a more nuanced and precise diagnostic tool for evaluating climate change impacts—particularly in regions such as the Arctic, where extreme values often drive systemic transformations.

The empirical results reveal a distinct pattern: in the Arctic, there is clear and robust evidence of warming that extends beyond the mean, with every quantile of the temperature distribution exhibiting an upward trend. In contrast, Antarctica shows no statistically significant trends across the distribution, indicating relative stability over the study period. In the Arctic, warming remains relatively steady until around 1960, after which a marked acceleration becomes evident across nearly all quantiles—except for the highest ones (*q90* and *q95*). When the analysis is extended to global temperatures, a similar acceleration pattern emerges, but in this case, it encompasses the entire distribution.

With regard to Arctic Amplification (AA), the study finds that this phenomenon remained relatively stable throughout most of the twentieth century, only beginning to intensify toward its end. Importantly, the amplification is not uniform across the Arctic temperature distribution. It is most pronounced at the mean and in all quantiles below the median. In the latter half of the century, amplification becomes increasingly evident in the upper quantiles, and by the century's end, it is observable across the entire distribution—except for the very highest quantiles (*q90* and *q95*).

The Arctic Amplification (AA) values estimated in this study are slightly below 2, closely aligning with the projections of climate models but falling below some recent observational estimates, which approach values near 4 (see Rantanen et al., 2022; Zhou et al., 2024). This discrepancy primarily stems from the higher global warming trend assumed in our analysis—exceeding 0.3°C per decade—whereas recent studies often adopt a lower trend, typically just under 0.2°C per decade. Methodologically, a key distinction lies in how amplification is calculated: either as a simple ratio of Arctic to global temperature increases or via regression of Arctic temperatures on global temperatures. The ratio-based approach complicates the construction of confidence intervals, particularly when the denominator is close to

zero. In contrast, the regression-based method allows for more straightforward statistical inference and is robust to both heteroskedasticity and serial correlation in the regression residuals (see Appendix for further details). Finally, our analysis is limited to land-based temperature data and does not incorporate oceanic regions.

A closer examination of the internal structure of Arctic Amplification reveals that it is largely driven by the lower quantiles of the temperature distribution. These lower quantiles correspond to winter temperatures in the high latitudes, which are crucial for processes such as sea ice formation. Thus, the study highlights the significant role that cold-season extremes play in shaping the overall pattern of Arctic warming and its amplification relative to the rest of the Globe.

In contrast to the Arctic, the scientific consensus on Antarctic climate change remains divided. Studies such as Comiso (2000), Trivedi (2002), Steig and Schmidt (2004), Steig et al. (2009), O'Donnell et al. (2011), Nicolas and Bromwich (2014), Turner et al. (2016), Easterbrook et al. (2016), and Singh and Polvani (2020) report conflicting trends. While the Antarctic Peninsula exhibits clear and consistent warming, other regions show evidence of cooling. Overall, Antarctic climate trends are weaker than those in the Arctic and vary depending on the season and time period analyzed. Climate models predict smaller warming trends in Antarctica, primarily due to the moderating influence of the Southern Ocean, which absorbs heat and delays surface temperature increases. Station geography also influences observed trends: significant warming has been recorded in West Antarctica, whereas cooling trends predominate across much of the rest of the continent. The limited and uneven distribution of observational data further complicates these analyses. Notably, the IPCC Sixth Assessment Report (2021), particularly Chapter CCP6, explores ecosystem effects and adaptation policies in polar regions but does not directly compare the warming processes in Antarctica and the Arctic (Constable et al., 2022). It states the unique geography, persistent ice sheet, oceanic isolation, and atmospheric circulation patterns collectively dampen its warming rate compared to the Arctic. Our station-based approach clearly finds evidence of no warming in Antarctica.

Several studies address the contrasting climate phenomena in the Arctic and Antarctic. Pithan and Mauritsen (2014), Salzmann (2017), Yamanouchi et al. (2020), Walsh (2021) and IPCC (2021) attribute the differences to distinct geographical and climatic characteristics. The Arctic, as a sea ice-covered ocean, is particularly vulnerable to feedback mechanisms (Serreze et al., 2007; Miller et al.,

2010). Conversely, Antarctica, a high-altitude landmass covered by ice and snow, experiences moderated surface warming due to the deep and slow-moving ocean currents that regulate its temperature (Cox et al., 2024). This results reflects the differences between East and West (e.g., East is high-altitude plateau ice sheet subject to limited ocean forcing, whilst West is lower-altitude marine-based ice sheets subject to stronger ocean forcing).

The main findings for the Arctic show both parallels and contrasts with global temperature trends. In both the Arctic and the world as a whole, all aspects of the temperature distribution —including average values and extremes— have increased over time. However, the way these changes have developed reveals important differences. Across the Globe, warming trends reached a peak around 1970. After that, the pace of increase largely leveled off, a pattern also noted by Beaulieu et al. (2024). The Arctic, however, tells a different story. While temperatures have risen at all levels, the coldest extremes (the lower quantiles) have warmed much more rapidly than the warmest extremes (the upper quantiles). This has led to a marked decrease in the interquartile range (iqr), meaning that the overall variability in Arctic temperatures has narrowed. In contrast, the global temperature distribution has shifted more uniformly: both the lower and upper quantiles have increased at similar rates, so the iqr has not changed significantly. Despite these differences, both the Arctic and the globe have seen an overall acceleration in warming compared to the whole sample period 1900-2019. Notably, while this acceleration affects all quantiles in the Globe, in the Arctic the upper quantiles (such as the 90th and 95th percentiles) have remained stable over time.

The work is designed as follows. Section 2 briefly presents the methodology used. The empirical application is divided into two sub-sections for the Arctic and the Antarctic and in each of them data and results for existence, acceleration and amplification are presented. A final section summarizes the main conclusions. An Appendix contains additional results and technical details of the AA calculation.

2 Quantitative Methodology

The methodology used in this paper grounds in the quantitative approach introduced in GG2020, where every characteristic (not only the average) of the temperature distribution is converted into a time series object. This allows us to define the important climate concepts in a testable format. For example, warming is defined as

an increasing trend in some of these distributional characteristics. More technically:

Definition 1. *(Warming): Warming is defined as the existence of an increasing trend in some of the characteristics measuring the central tendency or position (quantiles) of the temperature distribution.*[2]

Temperature is viewed as a functional stochastic process $X = (X_t(\omega), t \in T)$, where T is an interval in $\mathbb{R}$, defined in a probability space $(\Omega, \Im, P)$. A convenient example of an infinite-dimensional discrete-time process consists of associating $\xi = (\xi_n, n \in \mathbb{R}_+)$ with a sequence of random variables whose values are in an appropriate function space. This may be obtained by setting

$$X_t(n) = \xi_{tN+n},\ 0 \leq n \leq N,\ t = 0, 1, 2, ..., T \tag{1}$$

so $X = (X_t, t = 0, 1, 2, ..., T)$. The choice of the period or segment t will depend on the situation in hand. In our case, t will be the period of a year, and N represents cross-sectional observations.

Going back to the convenient example and adjusted notation ($X_t(n) = X_{tn}$ and n a natural number), the stochastic structure can be summarized in the following array:

$X_{00}(w) = \xi_0(w)$	$X_{01}(w) = \xi_1(w)$	. . .	$X_{0N}(w) = \xi_N(w)$	$C_0(w)$
$X_{10}(w) = \xi_{N+1}(w)$	$X_{11}(w) = \xi_{N+2}(w)$	. . .	$X_{1N}(w) = \xi_{2N}(w)$	$C_1(w)$
$X_{20}(w) = \xi_{2N+1}(w)$	$X_{21}(w) = \xi_{2N+2}(w)$	. . .	$X_{3N}(w) = \xi_{3N}(w)$	$C_2(w)$
.	.	. . .	.	.
.	.	. . .	.	.
.	.	. . .	.	.
$X_{T0}(w) = \xi_{(T-1)N+1}(w)$	$X_{T1}(w) = \xi_{(T-1)N+2}(w)$	. . .	$X_{TN}(w) = \xi_{TN}(w)$	$C_T(w)$

(2)

where the distributional characteristics ($C_t(w)$) represent the state mean, the state variance, the state kurtosis, the state quantiles, etc. To detect the existence of warming, that is to say, a trend component in a characteristic C_t of X_t we use the following test:

Definition 2. *(Practical trend test, TT): A characteristic C_t of a functional stochastic process X_t contains a trend if in the least square regression,*

$$C_t = \alpha + \beta * t + u_t,\ t = 1, ..., T, \tag{3}$$

[2]The trend —and, by extension, the warming— can be detected in any characteristic of the distribution. GG2025 define a typology of warming based on the significance of trends across various distributional characteristics.

$\beta = 0$ is rejected according with the t-statistic $t_{\beta=0}$ whose distribution under the null (null) is asymptotically normal.[3]

Notice that when C_t correspond to some characteristics measuring the central tendency or position (quantiles) an t years, the units of the slope coefficient β are Celsius degrees per year.

GG2020 shows that a simple $t_{test(\beta=0)}$ is able to detect most of the existing deterministic trends (polynomial, logarithmic, exponential, etc) and also the trends generated by any of the three standard persistent processes considered in the literature (see Müeller and Watson, 2008): (i) fractional or long-memory models ($1/2 < d < 3/2$); (ii) near-unit-root autoregressive (AR) models; and (iii) local-level models.

Several remarks are relevant with respect to this practical definition: (i) regression (3) has to be understood as the linear least square approximation of an unknown trend function $h(t)$ (see White, 1980); (ii) the parameter β is the *plim* of $\widehat{\beta}_{ols}$; (iii) if the regression (3) is the true data-generating process, with $u_t \sim I(0)$[4], then the OLS (ordinary least square (Ordinary Least Square) $\widehat{\beta}$ estimator is asymptotically equivalent to the GLS (Generalized Least Square) estimator (see Grenander and Rosenblatt, 1957) and the $t-test(\beta = 0)$ is *N(0,1)*; (iv) in practice, in order to test $\beta = 0$, it is recommended to use a HAC (Robust standard errors in the presence of heteroscedasticity and autocorrelation) version of $t_{\beta=0}$ (see Busetti and Harvey, 2008); and (v) this test only detects the existence of a trend but not the type of trend. Notice also that in (3) we could be totally agnostic about u_t being *I(0)* or *I(1)*. In this case following Perron and Yabu (2009) we can estimate the model by Feasible Generalized Least Squares and construct a similar *t-stat* of $\beta = 0$ that still will follow a *N(0,1)*. This method depends on a tuning parameter (how close is u_t of being *I(1)*). To avoid that, in this paper, we follow an alternative approach. We pre-test the temperature data for unit roots, once they are rejected we proceed as if u_t in 3 is *I(0)*.

For all these reasons, in the empirical applications we implement Definition 2 by estimating regression (3) using OLS and constructing a HAC version of $t_{\beta=0}$ (Newey

[3]More details of the properties of this test can being found in GG2020.

[4]An $I(1)$ process is the accumulation of an $I(0)$ process. Our definition of an I(0) process follows Johansen (1995). A stochastic process Y_t that satisfies $Y_t - E(Y_t) = \sum_{i=1}^{\infty} \Psi_i \varepsilon_{t-i}$ is called I(0) if $\sum_{i=1}^{\infty} \Psi_i z^i$ converges for $|z| < 1 + \delta$, for some $\delta > 0$ and $\sum_{i=1}^{\infty} \Psi_i \neq 0$, where the condition $\varepsilon_t \sim$ iid $(0, \sigma^2)$ with $\sigma^2 > 0$ is understood.

and West, 1987).

3 Warming Acceleration and Warming Amplification

In this section, we apply the methodology described previously to instrumental observations from the land Arctic polar circle (Arctic) and the Antarctic polar circle (Antarctic) using the database provided by the Climate Research Unit (CRU) that offers temperatures across the Globe and allows us to extract data from both poles. The Arctic and Antarctic polar circles are defined, respectively, as the land surface with latitude greater than 66.5 degrees and less than -66.5 degrees.

3.1 The Arctic

3.1.1 The Data

The Climatic Research Unit (CRU) provides monthly and annual temperature data for land and sea surfaces across both hemispheres, spanning the period from 1850 to the present. These data are collected from a wide network of meteorological stations distributed globally.[5] The original data are gridded at 5-degree resolution and normalized using the 1960–1990 average to compute temperature anomalies.[6] It should be pointed out that most of the stations used are land-based. Since there is roughly 50:50 proportion of land to ocean area, there is a large proportion of the Arctic that is not represented at all (the ocean).

We conducted our analysis using raw temperature data from meteorological stations, selecting only those located at latitudes higher than 66.5°N.[7] Globally, the total number of stations in the dataset is 10,296,[8] of which 356 are situated within

[5]HadCRUT4 is a global temperature dataset offering gridded temperature anomalies as well as hemispheric and global averages. CRUTEM4 and HadSST3 represent the land and ocean components, respectively. These datasets have been developed by the CRU (University of East Anglia) in collaboration with the Hadley Centre (UK Met Office), except for the sea surface temperature dataset, which was developed exclusively by the Hadley Centre. In this study, we use CRUTEM versions 4.6.0.0 and 5.0.1.0, which are publicly available at https://crudata.uea.ac.uk/cru/data/temperature/ (accessed 23/08/2020). Detailed methodology is presented in Jones et al. (2012), with an updated version in Morice et al. (2021).

[6]We have also utilized the Arctic Surface Air Temperature (SAT) database, yielding very similar results.

[7]This corresponds to the official definition of the Arctic Circle and it is the standard definition in the literature. However, Bekryaev et al. (2010) adopt a broader criterion, considering the Arctic as the region north of 60°N.

[8]Reduced to 9,908 after excluding 402 stations identified as having uncertain coordinates and marked as pending revision.

the Arctic Circle.[9] The number of active Arctic stations, however, varies significantly over time and across regions. The CRU dataset is compiled from multiple sources, some of which update their records intermittently. This is particularly relevant for polar data, as the collection of observations in such remote and harsh environments poses substantial logistical challenges.[10] Our review indicates that the maximum density of observations from Arctic stations in the CRU dataset occurs during the period 1960–2000. To evaluate the potential impact of this spatial-temporal variation on temperature trends, we computed annual average temperatures based on the stations reporting in each year. The results suggest that the range of variability for the Arctic Circle has remained relatively stable since the end of World War II.

This distribution of observational data motivated the selection of a temporally and spatially representative sample, allowing for the statistical identification of temperature trends with a high degree of confidence. To this end, we applied a rolling algorithm designed to identify the optimal sample based on two criteria: the number of stations and the number of consecutive years. A strict requirement was imposed: all selected stations must provide complete annual data throughout the study period. The final sample spans from 1950 to 2019 and includes 48 stations located within the Arctic Circle, as shown in Figure 1. Although this is the preferred sample, we conducted robustness checks using alternative periods to assess the stability of the results, including longer time frames.[11]

The decision to work with raw station data is closely tied to the objectives of our research, which requires high-frequency information—either in time or space—to capture the full distribution of temperatures and ensure the stability necessary for accurately estimating trends. The main drawback of using raw data is its limited spatial coverage. Nevertheless, this approach offers critical advantages: it preserves the integrity of the original observations, avoids potential biases introduced through constructed data (post-processed within a re-analysis framework), and maintains the consistency of station records across the sample period. Importantly, it also retains regional variability and removes dependence on grid resolution, interpolation techniques, or climate model assumptions.

[9] This number decreases to 340 after removing stations with implausible geographic coordinates.

[10] We are especially grateful to David Lister for his technical support.

[11] As shown in Figure A1, extending the sample to end in 2008 or 2012 increases the number of usable stations by approximately twofold. In this study, we prioritized temporal coverage over the number of stations, given the representativeness of the selected subset. Nonetheless, all calculations were replicated for the period 1950–2012, yielding very similar conclusions. Results are available upon request.

For these reasons, our approach is preferred over gridded datasets, which are commonly used and often supplemented by hybrid methods to fill gaps in sparse regions or reanalysis products derived from climate models. In the case of gridded data—both filled and unfilled—the absence of missing data in regions without observational input and the temporal variation in station location and number may introduce artificial trends. Moreover, interpolation methods tend to suppress variance, which poses a problem for studies focused on the heterogeneity of climate change (see Harris et al., 2020). With respect to global reanalysis datasets, while their utility for climate studies is widely acknowledged, they present limitations for our specific methodology. These include reduced sample size due to coverage restrictions, difficulties in maintaining consistent data frequency across time, and a strong dependence on model parameters. Additionally, the temporal stability of station coverage can significantly affect the stochastic properties of temperature series (Gadea et al., 2024). Hyncica and Huth (2020) examine discrepancies between station data and interpolated grid points, finding that such differences are especially pronounced in the tails of the distribution—precisely where our method focuses.

Several studies have highlighted that undercoverage bias may be particularly pronounced in polar regions due to sparse observational data in the HadCRUT4 temperature series, potentially resulting in a cool bias. Alternative datasets, such as GISTEMP (NASA's Goddard Institute for Space Studies Surface Temperature Analysis), UAH (University of Alabama in Huntsville satellite data), and NCEP/NCAR (National Centers for Environmental Prediction/National Center for Atmospheric Research reanalysis data), consistently indicate that the Arctic is warming at a faster rate than the global average. Additionally, both GISTEMP and NCEP/NCAR show accelerated warming in the Antarctic as well (Cowtan and Way, 2014). Chylek et al. (2022) compare multiple observational databases—including HadCRUT (Climatic Research Unit), GISTEMP, and NOAA (National Oceanic and Atmospheric Administration)—and, despite minor discrepancies among them, report broadly consistent periods of Arctic amplification. However, these amplification signals are notably more distinct when contrasted with those derived from climate models such as CMIP5, CMIP6, and the Ocean Model Intercomparison Project. Cohen et al. (2019) further emphasize the divergence in consensus between model simulations and observational evidence concerning Arctic amplification.[12]

[12]We have also conducted a benchmarking exercise using reanalysis data, comparing the results with those obtained from raw CRU station data. The reanalysis dataset employed corresponds to

The construction of distributional characteristics merits further explanation. Based on the selected Arctic sample and using monthly data, we construct a set of characteristics denoted by $C_t = (C_{1t}, C_{2t}, \ldots, C_{pt})$, representing a vector of p distributional statistics. These include the mean ($mean$), interquartile range (iqr), and a series of quantiles: $q05$, $q10$, $q20$, $q30$, $q40$, $q50$, $q60$, $q70$, $q80$, $q90$, and $q95$. A unit (defined as a month-station pair) is included only if complete data are available. The time-series objects C_t are computed annually based on all month-station units for that year. For the Arctic sample spanning 1950–2019, the total number of units is 408 across 48 stations, taking into account missing stations for a particular month.[13] The density of Arctic data is depicted in Figure 2, while the evolution of the distributional characteristics is shown in Figure 3. Figure A3 further illustrates the temporal stability of the selected stations.

To isolate and compare the effects of global warming in the Arctic, we conducted a parallel analysis for the entire Globe using the same data selection methodology. The density of this global dataset for the period 1950–2019 is presented in Figure 5, and the temporal evolution of quantiles is illustrated in Figure 6. This global sample includes 952 stations, producing a total of 9,402 valid units. An insightful exercise involves examining the relationship between the stations comprising the lowest global quantile (*q05*) and those located within the Arctic Circle. The *q05* quantile of the global dataset consists of 272 stations, whose geographic distribution—excluding four Antarctic stations—is displayed in Figure 4. Of the 48 Arctic stations, 41 (approximately 85%) fall within the *q05* quantile. However, the quantile also includes numerous stations located outside the Arctic Circle. Those Arctic stations not included in the lowest quantile are primarily located in Norway, with a few in Sweden, Russia, and Canada.[14] Conversely, extremely low temperatures are observed during winter months at considerably lower latitudes in countries such as the United States and Denmark.

the most recent version of ERA5 (ECMWF project), which includes land-monthly averaged data from 1950 to the present. The estimated temperature distribution trends derived from this dataset closely align with those obtained from the station data. Full results are available from the authors upon request.

[13]For the extended period 1950–2012, the figures increase to 721 units across 83 stations.

[14]It is worth noting that the Norwegian Lofoten Islands exhibit the most pronounced climatic anomaly globally in relation to latitude. Despite lying within the Arctic Circle, they experience relatively mild temperatures due to the influence of the Gulf Stream.

3.1.2 Warming Existence

Applying Definition 1 we can define Polar Warming (PW) as the existence of an increasing trend in some of the characteristics of the polar temperature distribution. Similarly, as in GG2020 we obtain the definition of Global Warming (GG).

The presence of a significant trend in polar temperature characteristics during the period 1950-2019 is tested by applying the proposed trend-test (TT) in regression (3).[15] This regression has been estimated by ordinary least squares with errors robust to the presence of heteroscedasticity and autocorrelation (OLS-HAC) and the results are displayed in Table 1 (sixth column). We have repeated the process for different previous and subsequent samples 1900-2019, 1910-2019, 1920-2019, 1930-2019, 1940-2019, 1950-2019, 1960-2019, 1970-2019 and 1990-2019 (see rest of the columns of Table 1). We will initially focus on the period 1950-2019.

The results show a significant trend in all characteristics. The trend is positive in all these time series except for the one measuring volatility, iqr, which have a significant negative trend. With respect to the rest, the mean has a trend coefficient of 0.0381, which implies an increase of almost 4 degrees in 100 years, and we find the highest positive trends in the lower quantiles. Notice that the trend coefficient of quantiles ranges from 0.0574 in quantile 20% ($q20$) to 0.0160 in quantile 95% ($q95$). It should be noted that this test only confirms the existence of a trend, and therefore warming, but says nothing about its nature. The analysis of the remaining periods offers interesting findings.

The conclusion is clear: Arctic temperatures have shown a clear warming trend since 1900, evident across mean temperatures and most quantiles of the temperature distribution. However, this warming has not been uniform or constant throughout the entire period. There seems to be a clear acceleration in the ongoing warming process no reaching a peak yet in most of the distributional characteristics except for the upper quantiles (90th and 95th percentiles) that has stabilized since 1990, suggesting potential changes in extreme warm temperatures. Furthermore, the negative and significant trend in iqr suggests a narrowing of the distribution and thus a reduction in variability (see Giesse et al. 2024). Davy and Griewank (2023) states that rapid Arctic warming is tightly linked to the retreat and thinning of summer sea ice, and so may be expected to weaken as the Arctic transitions to seasonal ice

[15] Before testing for the presence of trends in the distributional characteristics of Arctic polar circle data from CRU, we test for the existence of unit roots. The results reject this hypothesis (See Table A2 in the Appendix).

cover.

In summary, the structure of Arctic Warming has undergone notable changes over time. Since 1950, warming has been observed across all quantiles, with a more pronounced increase in the lower temperature quantiles relative to the upper ones. This pattern is reflected in a declining trend in the interquantile range (iqr). The presence of an acceleration in this process will be formally assessed in the next section.

We apply the same procedure (preliminary unit root tests and TT estimates[16]) to the database of global temperatures from the CRU and display in Table 2 the estimated trends for the different periods.[17]

Global temperatures have also shown a consistent warming trend since 1900, evident across both mean temperatures and all the quantiles of the temperature distribution. Although a strict comparison between the Arctic Warming and the Global Warming will be done in the amplification section, there are some extra differences worthwhile to mention:

- The greater intensity of the Arctic Warming process with respect to the Globe, which is also clearly reflected in Figure 7.
- Global Warming trends reached a peak around 1970. After 1970, warming rates stabilized across mean and quantiles in line with Beaulieu et al. (2024).
- Despite the post-1970 stabilization, there is evidence of an overall acceleration in the warming process when comparing recent trends to the entire 1900-2019 period. This acceleration will be subject to formal statistical testing for confirmation.
- The warming process appears to affect the temperature distribution relatively uniformly across most analyzed periods. There is no significant trend observed in the *iqr* for most periods suggesting that the shape of the global temperature distribution has remained relatively stable, with warming affecting lower and upper temperature quantiles similarly.

[16]The analysis of stationarity in GG2020.
[17]A detailed analysis of cross-sectional CRU temperature data can be found in GG2020.

3.1.3 Warming Acceleration

Figures 8 and 10 illustrate the evolution of temperatures in the Arctic and globally for selected characteristics: *mean*, *q05*, and *q95*. The findings demonstrate a similar trajectory of the warming process, albeit more pronounced within the Arctic polar circle compared to global temperatures. Notably, there are specific nuances that merit attention. A key observation is that the greater intensity of the warming process on average in the Arctic, relative to the Globe —a well-documented result in the literature— is primarily attributable to the more rapid increase in the trend of the lower quantiles below the median (e.g. *q05*), in the Arctic.

These results suggest a process of warming acceleration, which warrants formal statistical testing. Warming acceleration refers to an increase over time in the trend captured by the β coefficient in regression 3. To test this hypothesis, we applied a recursive sampling method, starting in 1900 and progressively expanding the sample. The detailed results, presented in Table 1 for all temperature characteristics and in Figure 6 for selected quantiles, provide robust evidence for an acceleration phenomenon across all relevant characteristics.

Definition 3. *(Warming Acceleration)*: *We define warming acceleration in a distributional temperature characteristic C_t between the periods $t_1 = (1, ..., s)$ and $t_2 = (s+1, ..., T)$ as occurring when, in the following two regressions:*

$$C_t = \alpha_1 + \beta_1 * t + u_t,\ t = 1, ..., s, ..., T, \tag{4}$$

$$C_t = \alpha_2 + \beta_2 * t + u_t,\ t = s+1, ..., T, \tag{5}$$

the trend slope in the second period exceeds that of the first: $\beta_2 > \beta_1$.

In practice, we implement this definition by testing the null hypothesis $\beta_2 = \beta_1$ against the alternative $\beta_2 > \beta_1$. An equivalent approach involves testing for a structural break at $t = s$. However, we favor the framework presented in Definition 3 because it enables us to establish T as a fixed benchmark reference period—such as a century or a millennium. This approach is especially valuable for long-term climate analyses, as it allows us to use T as a standard for comparison with shorter periods, ranging from *s+1* to T. The results and their significance are detailed in Tables 3 and 4 for the Arctic and the global context, respectively.[18]

[18]Two common approaches are typically employed to assess the presence of warming acceleration. The first approach (a) involves comparing trends across two consecutive subperiods—specifically, from t to t_1, and from t_1 to T. The second approach (b) compares the trend over the entire period

The formal acceleration tests, based on data from 1900–2019, confirm statistically significant warming acceleration in mean temperatures and most quantiles. The primary distinctions between Arctic and global warming acceleration are as follows:

- Global Warming acceleration appears to have commenced slightly earlier (circa 1950) compared to the Arctic (circa 1960).
- Unlike the Arctic, Global Warming acceleration is observable even in the upper quantiles (e.g., *q90* and *q95*).

To provide a more granular perspective, heat maps (Figures 9 and 11) illustrate the temporal evolution of trend coefficients by temperature characteristics, with finer temporal resolution after 1950. The scale ranges from -0.0653 to 0.1102, representing the minimum and maximum coefficient values across the datasets. Time spans from 1900 to 2019, with annual intervals after 1950. The maps use varying intensities of blue for negative values and a spectrum from green to red (passing through yellow and orange) for positive values. These visualizations vividly highlight the greater intensity of warming within the Arctic polar circle compared to global temperatures. This difference is particularly evident in the lower quantiles but is also present in the mean and other quantiles. These findings support a key motivation of this study: the discontinuity in warming impacts across the temperature distribution. If the observed average temperature increase is driven primarily by lower quantiles rather than upper quantiles, the associated consequences could be more severe.

The main conclusion is that Arctic Warming remained stable (i.e., without acceleration) until approximately 1960. Thereafter, clear warming acceleration is evident in the mean and all quantiles below *q90*. The delayed onset of acceleration (post-1960) suggests that this phenomenon may not be entirely attributable to natural causes or variability. Instead, external factors, such as increased global industrial activity and associated CO2 emissions, are likely contributors. Further investigation is required to understand the mechanisms underlying these divergent warming acceleration patterns between the Arctic and global scales.

t_1 from t to T with that observed from to T. Although both approaches yield equivalent conclusions regarding the presence of acceleration, approach (a) is more commonly adopted in the literature. In this study, however, we employ approach (b), as it allows us to designate T as a fixed benchmark reference period—such as a century or a millennium. This feature is particularly valuable for long-term climate analyses, as it facilitates consistent comparisons between the full period and shorter subperiods ranging from *s+1* to T.

Finally, we directly compare the two warming processes by examining the amplification experienced by the Arctic.

3.1.4 Warming Amplification

In this section, we test both Polar and Global Warming amplification using a double-slope framework. Specifically, we evaluate amplification in two contexts: (i) with respect to an external distribution and (ii) within a distribution's own characteristics. The following hypothesis is tested:

Definition 4. *(Warming Amplification with respect to the mean): We define warming amplification in a distributional characteristic C_t with respect to the mean as occurring when, in the following regression:*

$$C_t = \beta_0 + \beta_1 * mean_t + \epsilon_t, \tag{6}$$

the slope associated with the mean is greater than one: $\beta_1 > 1$.

When the average, $mean_t$, and C_t are derived from the same distribution, we refer to this as "local" or "internal" warming amplification. Conversely, if the mean originates from an external distribution, it is termed "external" warming amplification. This approach is asymptotically equivalent to the tests commonly employed in the literature (e.g., Rantanen et al., 2022), though slight differences may emerge in small samples. The equivalence and advantages of this regression-based test are detailed in the Appendix.

We apply this framework to three cases: (i) Arctic temperatures relative to global temperatures (Arctic-Global, or external amplification), (ii) Arctic temperatures within their own distribution (Arctic-Arctic, or local amplification), and (iii) global temperatures within their own distribution (Global-Global). Results are presented in Tables 5, 6, and 7, respectively.

The results for land Arctic amplification can be summarized as follows:

- AA has remained stable throughout most of the twentieth century, only beginning to intensify towards its end (Table 5). This finding contrasts with Davy and Griewank (2023), who argue that AA peaked in the early 2000s, and with England et al. (2021), who suggest it is a recent phenomenon.

- Notably, this amplification is not uniform across the entire Arctic temperature distribution. It is most pronounced in the average and in all quantiles below

the median. Lower quantiles (below the median) exhibit stronger amplification across all analyzed periods, always surpassing mean amplification. From another perspective, these findings are also consistent with those of Johannessen et al. (2016) and Chylek et al. (2022), who observed that AA exhibits seasonal variability, with its maximum values occurring in winter and minimum values in summer.

- During the latter half of the twentieth century, the amplification becomes evident in more of the upper quantiles, and by century's end, it is present in all quantiles except for the very highest (*q90* and *q95*).

- The values calculated for AA in this study are slightly below 2, which aligns closely with the results produced by climate models but is lower than some recent observational estimates that approach 4. This discrepancy is primarily due to the higher Global Warming trend assumed in this analysis—greater than 0.3°C per decade—whereas recent studies typically use a global trend just under 0.2°C per decade. Amplification estimates in this study are lower than those in some observational studies. However, they align more closely with climate model projections (e.g., Rantanen et al., 2022; Davy and Griewank, 2023; Chylek et al., 2022, 2023).

- A closer examination of the internal structure of AA (Table 6) reveals that it is largely driven by the lower quantiles of the temperature distribution. These lower quantiles correspond to winter temperatures in the high latitudes, which are crucial for processes such as sea ice formation.

- Thus, the study highlights the significant role that cold-season extremes play in shaping the overall pattern of Arctic Warming and its amplification relative to the rest of the Globe.

- At the global level (Table 7), our results reveal that amplification is not an Arctic-exclusive phenomenon. Instead, it extends from the 5th percentile, prominently observed in the Arctic, to the 20th percentile (Northern Europe) in global temperature distributions.

In summary, the amplification of temperature quantiles, particularly in colder regions and seasons, highlights the nuanced and multifaceted impacts of climate change. These effects are often obscured when focusing solely on changes in mean

temperatures. This underscores the importance of analyzing the full distribution of temperatures in climate change assessments and adaptation strategies. For a comprehensive review of AA mechanisms, see Previdi et al. (2021). Studies on its effects are discussed by Screen (2013), Cohen et al. (2019), Blackport and Screen (2020), and Isaksen and Ivanov (2022).

3.2 The opposite pole: the Antarctic

The strategy for station selection is consistent with previous approaches; however, data scarcity in Antarctica restricts the sample to the period 1960–2022, during which 67 units and 7 stations were selected. For a second analysis period, 1990–2022, focused on examining acceleration and robustness, the sample was expanded to 114 units and 11 stations. To establish a comparative framework, similar samples were drawn for the Arctic and the Globe. The geographical distribution of these areas is illustrated in Figure 12, while the selection process is detailed in Figure A2.

Antarctica presents significant challenges due to the limited availability of long-term meteorological observations and their uneven spatial distribution. Fewer than twenty permanent stations exist, with only two located in the interior, both of which lack consistent data continuity. As a result, analyzing long-term station-based trends in Antarctic temperatures remains infeasible.

Table 8 highlights the stark contrast in temperature trends between the two poles over the period 1960–2022. For the South Pole, all trends are statistically non significant at 1%. In contrast, Arctic stations display trends that are both stronger in magnitude and statistically significant. Given the absence of warming across the analyzed Antarctic periods, further testing for acceleration or amplification phenomena is not warranted. Figures 13 and 14 present a comparative overview of temperature trends in Antarctica, the Arctic, and the Globe, underscoring the pronounced asymmetry between the poles —a phenomenon widely documented in the literature (e.g., Salzmann, 2017).

The scarcity and uneven geographical distribution of observational data largely account for these results. Figure 15 offers a detailed analysis of temperature data from candidate stations during 1960–1990. The upper panel shows greater data discontinuity among western stations compared to eastern ones, while the lower panel reveals that temperature increases (normalized by longitude) are higher in the west than in the east, averaging 0.16 and -0.068, respectively. Most selected stations, chosen for data continuity, are located on the eastern slope of Antarctica, a region

characterized by less warming —or even cooling. These findings are consistent with previous research suggesting that relatively milder areas, such as western Antarctica and regions closer to South America, are experiencing warming, whereas the eastern zone has shown no significant temperature changes over the past 50 years and, in some cases, evidence of cooling. Recent studies, including one based on aerial photography, even indicate a long period of glacier stability and growth in East Antarctica (Dømgaard et al., 2024).

These observations complicate drawing definitive conclusions about the impact of greenhouse gases. Antarctica appears to be warming along its edges while simultaneously cooling in its interior. Reflecting this complexity, the IPCC's Fourth Assessment concluded that anthropogenic temperature changes had not been detected on the continent, primarily due to limited data collection. Similarly, the Sixth Assessment (2021) reported no significant trend in Antarctic sea ice area between 1979 and 2020, attributing this to regionally opposing trends and high internal variability. The report also underscored the importance of Southern Ocean processes in regulating deep ocean temperatures.

Although variability in temperature patterns complicates scientific assessments, studies by Thompson and Solomon (2002) and Shindell and Schmidt (2004) provide explanations for observed cooling trends between the 1970s and 2000. Long-term analyses, such as those by Mayewski et al. (2009) and Convey et al. (2009), examine the broader Antarctic climate system and offer comparisons with the Arctic. O'Donnell et al. (2011) and Easterbrook et al. (2016) demonstrate cooling dominance across much of East Antarctica and refute the findings of Steig et al. (2009), who reported warming across the entire continent. Similarly, Turner et al. (2016) argue that the absence of warming in Antarctica during the 21st century aligns with natural variability, while Singh and Polvani (2020) attribute the continent's low climate sensitivity to the influence of its ice sheet topography. More recently, Casado et al. (2023) reaffirmed West Antarctica's vulnerability to warming and found evidence of a stronger amplification effect than predicted by climate models. These findings contrast with Monaghan et al. (2008), who claimed that climate models often overestimate warming in Antarctica by a factor of three, despite accurately simulating climate trends on other continents.

In conclusion, while there is no consensus on the extent of climate change (warming) in Antarctica, many studies suggest that its impact is smaller compared to the rest of the planet. our analysis of Antarctica, based on the available data, reveals

no significant evidence of warming or related phenomena such as acceleration or amplification. The limited availability of observational data necessitates reliance on indirect methods, such as ice core analysis and aerial photography, alongside climate models and observational records. Consequently, understanding climate change on this continent remains a significant challenge for climate scientists.

4 Concluding remarks

This paper has a strong methodological orientation, offering quantitative tools to analyze the dynamics of climate change. Our findings provide a robust description of the warming processes affecting the polar regions, with all results subjected to robust testing. By shifting focus from averages to distributional trends, this work provides a more precise tool for diagnosing climate change impacts, particularly in regions like the Arctic where extremes drive systemic shifts.

Regarding the land Arctic, our key conclusions are as follows:

- Positive station-based Trends Across Distributional Characteristics: There is a clear positive trend across all distributional characteristics of temperature, not only the average, indicating consistent warming.
- Singular Warming Processes: There are clear differences with the Globe.
- Stronger Trends in Lower Quantiles: The lower quantiles exhibit larger trends than both the mean and upper quantiles, suggesting that the coldest temperatures are warming faster than the rest of the distribution.
- Decreasing Variability: *iqr* has a negative trend, as lower temperatures are converging toward the median more rapidly than higher temperatures.

These findings are consistent with the temperature trends observed in the Globe, though the magnitude is notably different. The Arctic is warming at a rate several times higher than the Globe average, and we find strong evidence that this warming is accelerating, more so than at the global scale. However, there is a key distinction: while all Globe temperature quantiles show signs of accelerated warming, in the Arctic, the upper quantiles (*q90* and *q95*) do not display this acceleration. Moreover, in contrast to the pattern observed in the Arctic, temperature variability in the Globe remains stable over the study period, with no significant trend detected in the interquartile range (*iqr*). Our analysis also highlights unique local and external

amplification effects within the Arctic. Notably, our results on Arctic amplification are in agreement with results from climate model simulations.

The Arctic is a highly complex and sensitive system, responding significantly even to minor temperature changes. This sensitivity has profound implications due to the system's reliance on the freezing point of water. Each summer, temperatures push the system toward the liquid phase, and each winter, it returns to the solid phase. While a degree or two of warming may have minimal perceptible effects in tropical regions, a similar increase in the Arctic can lead to transformative changes, particularly when temperatures shift from just below to just above the freezing point.

In contrast, our analysis of Antarctica, based on the available data, reveals no significant evidence of warming or related phenomena such as acceleration or amplification. These findings contribute to the ongoing scientific debate regarding Antarctica's temperature trends and underscore the stark differences in how the two poles respond to climate change. This highlights not only the geographical opposition of the poles but also their contrasting climatic responses.

However, it is essential to qualify this conclusion by acknowledging the disparities in data quality and coverage between the Arctic and Antarctic. The scarcity and heterogeneity of Antarctic observations limit the robustness of analyses, emphasizing the need for improved data collection in this region.

Our analysis is based on instrumental monthly observations from stations exhibiting stable behavior throughout the sample period. In future research, we plan to apply the same methodology to climate model outputs. This will allow us to assess how the spatio-temporal sparsity of weather stations in the historical record may influence model results. Additionally, it will be interesting to examine whether the findings differ across climate models and, consequently, which models most accurately reproduce real-world phenomena.

References

[1] Beaulieu, C., Gallagher, C., Killick, R., Lund, R, Shi, X. 2024. A recent surge in global warming is not detectable yet. Communications earth & environment. 5:576.

[2] Bekryaev, R.V., Polyakov, I.V., Alexeev, V.A., 2010. Role of polar amplification in long term surface air temperature variations and modern Arctic Warming.

J. Climate 23, 3888-3906.

[3] Blackport, R., Screen, J.A. 2020. Weakened evidence for mid-latitude impacts of Arctic warming. Nat. Clim. Chang. 10, 1065–1066.

[4] Brocka, W.A., J. Miller, J.I. 2004. Polar amplification in a moist energy balance model: A structural econometric approach to estimation and testing. Journal of Econometrics 245(1-2), 105885.

[5] Busetti, F., Harvey, A. 2008. Testing for trend. Econometric Theory 24, 72-87.

[6] Casado, M., Hebert, R., Faranda, D., Landais, A., 2023. The quandary of detecting the signature of climate change in Antarctica. Nature Climate Change 13, 1082–1088.

[7] Chylek, P., Folland, C., Klett, J.D., Wang, M., Hengartner, N. Lesins, G., Dubey, M.K. (2022). Annual Mean Arctic Amplification 1970–2020: Observed and Simulated by CMIP6 Climate Models Geophysical Research Letters Volume 49, 13 e2022GL099371.

[8] Chylek, P., Folland, C., Klett, J.D., Lesins, G., Dubey, M.K. 2023. Arctic Amplification in the Community Earth System Models (CESM1 and CESM2). Atmosphere 14, 820.

[9] Cohen, J., Zhang, X., Francis, J., Jung, T., Kwok, R., Overland, J., Smith, D., 2018. Arctic change and possible influence on mid-latitude climate and weather: A US CLIVAR white paper (No. 2018-1). (K. Uhlenbrock, Ed.). Washington, DC: U.S. CLIVAR Project Office. doi:10.5065/D6TH8KGW

[10] Cohen, J. et al. 2019. Divergent conensuses on Arctic amplification influence on midlatitude server winter weather. Nature Climate Change https://doi.org/10.1038/s41558-019-0662-y.

[11] Comiso, J.C., 2003. Warming Trends in the Arctic from Clear Sky Satellite Observations. Journal of Climate 16, 3498-3510.

[12] Comiso, J.C., Hall, D.K., 2014. Climate trends in the Arctic as observed from space. WIREs Climate Change 5, 389–409.

[13] Constable, A.J., S. Harper, J. Dawson, K. Holsman, T. Must onen, D. Piepenburg, and B. Rost, 2022: Cross-Chapter Paper 6: Polar Regions. In: Climate Change 2022: lmpacts, Adaptation and Vulnerability. Contribution of Working Group 11 to the Six th Assessment Report of the lntergovernmental Panel on Climate Change [H.-0. Piirtner, D.C. Roberts, M. Tignor, E.S. Poloczanska, K. Mintenbeck, A. Alegría, M. Craig, S. Langs dorf, S. Liisc hke, V. Miiller, A. Okem, B. Rama (eds.)]. CambridgeUniversit y Press,Cambridge,UK and New York, NY, USA, pp. 2319- 2368.

[14] Convey, P, Bindschadler, R., di Prisco, G., Fahrbach, E., Gutt, J., Hodgson, D.A., Mayewski, P.A., Summerhayes, C.P., Turner, J. 2009. Antarctic climate change and the environment. Antarctic Science 21 (6), 541-563.

[15] Cowtan, K., Way, R. G. 2014. Coverage bias in the HadCRUT4 temperature series and its impact on recent temperature trends. Quarterly Journal of the Royal Meteorological Society, 140(683), 1935–1944.

[16] Chapman, S.C., Stainforth, D.A., Watkins, N.W. (2023). On estimating local long-term climate trends. Phil Trans R Soc A 371, 20120287.

[17] Davy, R., Griewank, Ph. 2023. Arctic amplification has already peaked. Environ. Res. Lett. 18, 084003.

[18] Dickey, D.A., Fuller, W.A., 1979. Distribution of the estimators for autoregressive time series with a unit root. Journal of the American Statistical Association 74, 427-431.

[19] Dømgaard, M., Schomacker, A., Isaksson, E., Millan, R., Huiban, F., Dehecq, A., Fleischer, A., Moholdt, G., Andersen, J.K., Bjørk, A.A.. 2024. Early aerial expedition photos reveal 85 years of glacier growth and statility in East Antarctica. Nature Communications 15, 4-446.

[20] Donat, M.G., Alexander, L.V. 2012. The shifting probability distribution of global daytime and night-time temperatures. Geophysical Research Letters 39(14).

[21] Easterbrook, D.J. 2016. Chapter 7 - Evidence That Antarctica Is Cooling, Not Warming in Evidence-Based Climate Science (Second Edition), 123-136.

[22] England, M. R., Eisenman, I., Lutsko, N. J., Wagner, T. J. W. 2021. The recent emergence of Arctic Amplification. Geophysical Research Letters, 48, e2021GL094086.

[23] Francis, J.A., S.J.Vavrus, 2012. Evidence linking Arctic amplification to extreme wather in mid-latitudes. Geophisical Research Letters 39. L06801.

[24] Gadea-Rivas, M.D., Gonzalo, J., 2020. Trends in distributional characteristics: Existence of global warming. Journal of Econometrics 214, 153-174.

[25] Gadea, M.D., Gonzalo, J., Ramos, A. 2024. Trends in Temperature Data: Microfundations of their Nature. Economic Letters 244, 111992.

[26] Gadea, M.D, Gonzalo J (2025) Climate change heterogeneity: A new quantitative approach. PLOS ONE 20(1): e0317208. https://doi.org/10.1371/journal.pone.0317208

[27] Giesse1, C., Notz, D., Baehr, J. 2024. The Shifting Distribution of Arctic Daily Temperatures Under Global Warming. Earth's Future 12, e2024EF004961.

[28] Gillett, N.P., Thompson, D.W.J 2003. Simulation of Recent Southern Hemisphere Climate Change. Science 302 (563), 273-275.

[29] Greene, Ch., Pershing, A.J., Cronin, T.M., Ceci, N. 2008. Arctic Climate Change and Its Impacts on the Ecology on the North Atlantic. Ecology 89(11), S24-S38.

[30] Grenander, U., Rosenblatt, M. 1957. Statistical Analysis of Stationary Time Series. New York: Wiley 1957.

[31] Harris, I., Osborm, T.J., Jones, P.D., Lister, D.H. 2020. Version 4 of the CRU TS Monthly High-Resolution Gridded Multivariate Climate Dataset. Sci Data 7, 109.

[32] Heuzé, C., Jahn, A. 2024. The first ice-free day in the Arctic Ocean could occur before 2030. Nat Commun 15, 10101. https://doi.org/10.1038/s41467-024-54508-3

[33] Hynčica, M. Huth, R. 2020. Gridded versus station temperatures: Time evolution of relationships with atmospheric circulation. Journal of Geophysical Research: Atmospheres 125, 20.

[34] Isaksen, K., Nordli, Ø., Ivanov, B. 2022. Exceptional warming over the Barents area. Scientific reports 12, 9371.

[35] Ji, F., Wu, Z., Huang, J. et al. 2014. Evolution of land surface air temperature trend. Nature Clim Change 4,462-466.

[36] IPCC, 2021: Climate Change 2021: The Physical Science Basis. Contribution of Working Group I to the Sixth Assessment Report of the Intergovernmental Panel on Climate Change [Masson-Delmotte, V., P. Zhai, A. Pirani, S.L. Connors, C. Péan, S. Berger, N. Caud, Y. Chen, L. Goldfarb, M.I. Gomis, M. Huang, K. Leitzell, E. Lonnoy, J.B.R. Matthews, T.K. Maycock, T. Waterfield, O. Yelekçi, R. Yu, and B. Zhou (eds.)]. Cambridge University Press, Cambridge, United Kingdom and New York, NY, USA, 2391.

[37] IPCC, 2022. Constable, A.J., S. Harper, J. Dawson, K. Holsman, T. Mustonen, D. Piepenburg, and B. Rost, 2022: Cross-Chapter Paper 6: Polar Regions. In: Climate Change 2022: Impacts, Adaptation and Vulnerability. Contribution of Working Group II to the Sixth Assessment Report of the Intergovernmental Panel on Climate Change [H.-O. Pörtner, D.C. Roberts, M. Tignor, E.S. Poloczanska, K. Mintenbeck, A. Alegría, M. Craig, S. Langsdorf, S. Löschke, V. Möller, A. Okem, B. Rama (eds.)]. Cambridge University Press, Cambridge, UK and New York, NY, USA, pp. 2319–2368.

[38] Johannessen, O.M., et al., 2016. Surface air temperature variability and trends in the Arctic: new amplification assessment and reginalisation. Tellus, Series A, Dinamic Meterology and Oceanography. 68, 28234, http://dx.doi.org/10.3402/tellusa.v68.28234.

[39] Langen, P.L., Alexeev, V.I., 2007. Polar amplification as a preferred response in an idealized aquaplanet GCM. Clim. Dyn. 29, 305–317.http://dx.doi.org/10.1007/s00382-006-0221-x.

[40] Lui, J., Wang, X., Wu, D. Wang, X. 2024. The historical to future linkage of Arctic amplification on extreme precipitation over the Northern Hemisphere using CMIP5 Aand CMIP6 models. Advance in Climate Change Research, forthcoming. https://doi.org/10.1016/j.accre.2024.07.008.

[41] McBean, G., Genrikh, A., Deliang, Ch., Førlan, E., Fyfe, J., Groisman, P. King, R., Melling, R., Vose, R., Whitfgield, P. 2005. Arctic Climate: Past and Present

in Arctic Climate Impact Assessment, Chap. 2, 21-60, Cambridge University Press, Cambridge, U.K.

[42] Matthes, H., Rinke, A. Dethloff, 2015. Recent changes in Arctic temperature extremes: warm and cold spells during winter and summer. Environ. Res. Lett. 10, 114020.

[43] Mayewski,P. A. , Meredith, M. P., Summerhayes, C. P., Turner,J., Worby,A., Barrett,P. J. , Casassa,G., Bertler, N. A. N., Bracegirdle,T., Naveira Garabato, A. C., Bromwich,D., Campbell,H., Hamilton, G. S., Lyons,W. B., Maasch,K. A., Aoki,S., Xiao,C., Tas van Ommen, 2009. State of the Antarctic and Sourhern Ocean Climate System. Review of Geophysics 47 (1).

[44] Miller, G.H., Alley, R.B., Brigham-Grette J., Fitzpatrick, J.J., Polyak, L., Serreze, M.C., White,J.W.C., 2010. Arctic amplification: can the past constrain the future? Quaternary Science Reviews 2 1779-1790.

[45] Monaghan, A., Bromwich, D.H., Schneider, .P. 2008. Twentieth century Antarctic air temperature and snowfall simulations by IPCC climate models. Geophysical Research Letters 35. L07502.

[46] Morice, C. P., Kennedy, J. J., Rayner, N.A., Winn, J. P., Hogan, E., Killick, R. E.,et al. 2021. An updated assessment ofnear-surface temperature change from 1850: the HadCRUT5 data set. Journal of Geophysical Research: Atmospheres,126, e2019JD032361. https://doi.org/10.1029/2019JD032361.

[47] Müeller, U.K., Watson, M. 2008. Testing models of low-frequency variability. Econometrica 7, 979-1016.

[48] Newey W.K., West, K.D. 1987. A Simple positive semi-definite, heterekodasticity and autocorrelation consistent covariance matrix. Econometrica 55, 703-708.

[49] Nicolas, J. P., Bromwich, D. H. 2014. New reconstruction of Antarctic near-surface temperatures: Multidecadal trends and reliability of global reanalyses. Journal of Climate 27, 8070-8093.

[50] O'Donnell, R., Lewis, N., McIntyre, S., Condon, J. 2011. Improved Methods for PCA-Based Reconstructions: Case Study Using the Steig et al. (2009) Antarctic Temperature Reconstruction, 2099-2115.

[51] Perrie, W., Long, Z., Hung, H., Cole, A. Steffen, A., Dastoor, A., Durnford, D., Ma, J., Bottenheim, J.W., Netcheva, S., Staebler, Drummond, J.R., O'Neill, N.T., 2012. Selected topics in arctic atmosphere and climate. Climatic Change DOI 10.1007/s10584-012-0493-6.

[52] Perron, P., Yabu, T. 2009. Testing for Shifts in Trend With an Integrated or Stationary Noise Component. Journal of Business & Economic Statistics 27(3), 369-96.

[53] Pithan, F., Mauritsen, T. 2014. Arctic amplification dominated by temperature feedbacks in contemporary climate models. Nature Geoscience, 7, 181–184.

[54] Polyakov, I.V., Bekryaev, R.V., Alekseev, G.V., Bhatt, U.S., Colony, R.L., Johnson, M.A., Maskshtas, A.P., WALSH, D. 2003. Variability and trends of air temperature and pressure in the maritime Arctic, 1875–2000. J. Climate, 16, 2067-2077.

[55] Previdi, M., Smith, K.L, L.M. Polvani, 2021. Arcti amplification of climate change: a review of underlying mechanisms. Environmental Research Letters 16, 093003.

[56] Przybylak, R., 2007. Recent air-temperature changes in the Arctic. Annals of Glaciology 46, 316-324.

[57] Rantanen, M., Karpechko1, A.Y., Lipponen, A., Nordling1, K., Hyvärinen, O., Ruosteenoja, K., Vihma, T., Laaksonen, A.. 2022. Athe Arctic has warmed nearly four times faster than the globe since 1979. Communications Earth & Environment. https://doi.org/10.1038/s43247-022-00498-3

[58] Reich, B.J., 2012. Spatiotemporal quantile regression for detecting distributional changes in environmental processes. Journal of the Royal Statistical Society Series C, Royal Statistical Society 61(4), 535-553.

[59] Salzmann, M. 2017. The polar amplification asymmetry: role of Antarctic surface height. Earth Syst. Dynam. 8, 323-336.

[60] Serreze M.C., Walsh, J.E., Chapin III, F.S.m Osterkamp, T., Dyurgerov, M., Romanovsky, V., Oechel, W.C., Morison, J., Zhang, T., Barry, R.G., 2000. Observational Evidence of Recent Change in the Northern High-Latitude Environment. Climatic Change 46, 159-207.

[61] Serreze M.C., Barry, R.G., 2011. Processes and impacts of Arctic amplification: A research synthesis. Global and Planetary Change 77, 85–96.

[62] Screen, J.A. 2013. Incluence of Arctic sea ice on European summer precipitation. Environmental Research Letters 8, 044015. doi:10.1088/1748-9326/8/4/044015

[63] Shindell, T., Schmidt, G.A. 2004. Southern Hemisphere climate response to ozone changes and greenhouse gas increases,Geophys. Res. Lett.,31, L18209.

[64] Singh, R.K., Maheshwari, M., Oza, S.R., Kumar , R., 2013. Long-term variability in Arctic sea surface temperatures. Polar Science 7, 233-240.

[65] Singh, H.A., Polvani; L.M. 2020. Low Antarctic continental climate sensitivity due to high ice sheet orography. Climate and Atmospheric Science 39.

[66] Shindell, T., Schmidt, G.A. 2004. Southern Hemisphere climate response to ozone changes and greenhouse gas increases,Geophys. Res. Lett.,31, L18209.

[67] Singh, R.K., Maheshwari, M., Oza, S.R., Kumar , R., 2013. Long-term variability in Arctic sea surface temperatures. Polar Science 7, 233-240.

[68] Steig, E. J., Schneider, D. P., Rutherford, S. D., Mann, M. E., Comiso, J. C., Shindell, D. T. 2009. Warming of the Antarctic ice-sheet surface since the 1957 International Geophysical Year. Nature 457 (7228), 459-462.

[69] Steig, E., Schmidt, G. 2004. Antarctic cooling, global warming?. Real Climate.

[70] Steele, M., Ermold, W., Zhang, J., 2008. Arctic Ocean surface warming trends over the past 100 years. Geophysical Research Letters 35, L02614.

[71] Thompson, D.W.J., Solomon, S. 2002. Interpretation of Recent Southern Hemisphere Climate Change. Science 296 (5569), 895-899.

[72] Trivedi, B.P. 2002. Antarctica Gives Mixed Signals on Warming. National Geographic.

[73] Tuomenvirta, H.,Alexandersson, H., Drebs, A., Frich, P., Nordli, P.O., 2000. Trends in Nordic and Arctic Temperature Extremes and Ranges. Journal of Climate.

[74] Turner, J., Lu, H., White, I., King, J.C., Phillips, T., Hosking, J.S., Bracegirdle, T.J., Gareth, J. M., Mulvaney, R., Pranab, D. 2016. Absence of 21st century warming on Antarctic Peninsula consistent with natural variability. Nature 535, 411-415.

[75] Walsh, J.E. 2020. Arctic Climate Change, Variability, and Extremes in Yang, D., Kane, D.L. (eds.) Arctic Hydrology, Permafrost and Ecosystems. Springer Link.

[76] Wang,X., Key,J.,Liu,Y., Fowler,Ch., Maslanik, J, Tschudi, M., 2011. Arctic Climate Variability and Trends from Satellite Observations. Advances in Meteorology.

[77] White, H. 1980. Using least square to approximate unknown regression function. International Economic Review 21, 149-170.

[78] Yamanouchi, T., 2011. Early 20th century warming in the Arctic: A review. Polar Science 5, 53-71.

[79] Zhou, W., Leung, L.R., Lu, J. (2024) Steady threefold Arctic amplification of externally forced warming masked by natural variability. Nat. Geosci. 17, 508–515.

5 Tables

Table 1
OLS slope linear trend estimates (CRU monthly station data, Arctic)

names/periods	1900-2019	1910-2019	1920-2019	1930-2019	1940-2019	**1950-2019**	1960-2019	**1970-2019**	1980-2019	**1990-2019**
mean	0.0181	0.0174	0.0128	0.0170	0.0256	**0.0381**	0.0519	**0.0595**	0.0689	**0.0802**
	(0.0000)	(0.0003)	(0.0225)	(0.0065)	(0.0007)	(0.0000)	(0.0000)	(0.0000)	(0.0000)	(0.0000)
iqr	-0.0062	-0.0047	-0.0072	-0.0094	-0.0146	**-0.0286**	-0.0356	**-0.0407**	-0.0416	**-0.0473**
	(0.0607)	(0.2762)	(0.2380)	(0.2670)	(0.1157)	(0.0003)	(0.0000)	(0.0002)	(0.0103)	(0.0930)
q5	0.0324	0.0249	0.0111	0.0331	0.0297	**0.0497**	0.0618	**0.0620**	0.0492	**0.0898**
	(0.0096)	(0.0663)	(0.3070)	(0.0074)	(0.0367)	(0.0000)	(0.0000)	(0.0000)	(0.0030)	(0.0000)
q10	0.0341	0.0336	0.0143	0.0305	0.0401	**0.0565**	0.0690	**0.0836**	0.0809	**0.1297**
	(0.0044)	(0.0060)	(0.1635)	(0.0076)	(0.0032)	(0.0000)	(0.0000)	(0.0000)	(0.0000)	(0.0000)
q20	0.0274	0.0268	0.0177	0.0228	0.0395	**0.0574**	0.0715	**0.0908**	0.1078	**0.1431**
	(0.0005)	(0.0026)	(0.0561)	(0.0490)	(0.0010)	(0.0000)	(0.0000)	(0.0000)	(0.0000)	(0.0000)
q30	0.0195	0.0192	0.0173	0.0229	0.0364	**0.0537**	0.0730	**0.0879**	0.1076	**0.1123**
	(0.0000)	(0.0001)	(0.0206)	(0.0273)	(0.0107)	(0.0002)	(0.0000)	(0.0000)	(0.0000)	(0.0000)
q40	0.0166	0.0180	0.0162	0.0153	0.0304	**0.0502**	0.0732	**0.0793**	0.0990	**0.0966**
	(0.0002)	(0.0002)	(0.0095)	(0.0354)	(0.0046)	(0.0006)	(0.0000)	(0.0000)	(0.0000)	(0.0002)
q50	0.0169	0.0174	0.0131	0.0142	0.0227	**0.0385**	0.0610	**0.0632**	0.0772	**0.0650**
	(0.0000)	(0.0002)	(0.0063)	(0.0123)	(0.0012)	(0.0002)	(0.0000)	(0.0000)	(0.0000)	(0.0035)
q60	0.0141	0.0152	0.0133	0.0151	0.0209	**0.0272**	0.0410	**0.0486**	0.0573	**0.0607**
	(0.0000)	(0.0000)	(0.0017)	(0.0031)	(0.0000)	(0.0003)	(0.0000)	(0.0000)	(0.0000)	(0.0001)
q70	0.0123	0.0139	0.0129	0.0165	0.0202	**0.0260**	0.0360	**0.0413**	0.0474	**0.0594**
	(0.0000)	(0.0010)	(0.0123)	(0.0003)	(0.0001)	(0.0000)	(0.0000)	(0.0000)	(0.0000)	(0.0000)
q80	0.0120	0.0104	0.0106	0.0144	0.0189	**0.0275**	0.0353	**0.0462**	0.0566	**0.0678**
	(0.0001)	(0.0012)	(0.0165)	(0.0005)	(0.0005)	(0.0000)	(0.0000)	(0.0000)	(0.0000)	(0.0000)
q90	0.0104	0.0101	0.0046	0.0059	0.0115	**0.0164**	0.0244	**0.0230**	0.0342	**0.0287**
	(0.0002)	(0.0004)	(0.1762)	(0.0862)	(0.0006)	(0.0000)	(0.0000)	(0.0028)	(0.0000)	(0.0036)
q95	0.0098	0.0058	0.0015	0.0047	0.0149	**0.0160**	0.0244	**0.0252**	0.0366	**0.0315**
	(0.0005)	(0.0575)	(0.6502)	(0.2585)	(0.0002)	(0.0009)	(0.0000)	(0.0040)	(0.0000)	(0.0020)

Notes: OLS estimates and HAC $t_{\beta=0}$ p-values in brackets, from regression: $C_t = \alpha + \beta * t + u_t$.

Table 2
OLS slope linear trend estimates (CRU monthly station data, Globe)

names/periods	1900-2019	1910-2019	1920-2019	1930-2019	1940-2019	**1950-2019**	1960-2019	**1970-2019**	1980-2019	**1990-2019**
mean	0.0122	0.0124	0.0132	0.0156	0.0200	**0.0245**	0.0289	**0.0326**	0.0341	**0.0320**
	(0.0000)	(0.0000)	(0.0000)	(0.0000)	(0.0000)	(0.0000)	(0.0000)	(0.0000)	(0.0000)	(0.0000)
iqr	0.0013	0.0009	-0.0006	-0.0020	-0.0049	**-0.0044**	-0.0038	**0.0006**	-0.0018	**0.0105**
	(0.1688)	(0.2780)	(0.3520)	(0.0953)	(0.0009)	(0.0098)	(0.0922)	(0.4332)	(0.3612)	(0.0935)
q5	0.0177	0.0199	0.0210	0.0316	0.0375	**0.0450**	0.0432	**0.0418**	0.0334	**0.0195**
	(0.0000)	(0.0000)	(0.0000)	(0.0000)	(0.0000)	(0.0000)	(0.0000)	(0.0000)	(0.0122)	(0.1364)
q10	0.0139	0.0145	0.0169	0.0252	0.0367	**0.0425**	0.0455	**0.0470**	0.0452	**0.0339**
	(0.0000)	(0.0000)	(0.0000)	(0.0000)	(0.0000)	(0.0000)	(0.0000)	(0.0000)	(0.0000)	(0.0220)
q20	0.0121	0.0124	0.0141	0.0177	0.0245	**0.0273**	0.0336	**0.0321**	0.0384	**0.0307**
	(0.0000)	(0.0000)	(0.0000)	(0.0000)	(0.0000)	(0.0000)	(0.0000)	(0.0000)	(0.0000)	(0.0059)
q30	0.0111	0.0112	0.0123	0.0152	0.0195	**0.0238**	0.0272	**0.0304**	0.0343	**0.0266**
	(0.0000)	(0.0000)	(0.0000)	(0.0000)	(0.0000)	(0.0000)	(0.0000)	(0.0000)	(0.0000)	(0.0008)
q40	0.0100	0.0098	0.0099	0.0120	0.0145	**0.0194**	0.0232	**0.0311**	0.0323	**0.0303**
	(0.0000)	(0.0000)	(0.0000)	(0.0000)	(0.0000)	(0.0000)	(0.0000)	(0.0000)	(0.0000)	(0.0000)
q50	0.0104	0.0105	0.0110	0.0117	0.0142	**0.0187**	0.0232	**0.0278**	0.0318	**0.0310**
	(0.0000)	(0.0000)	(0.0000)	(0.0000)	(0.0000)	(0.0000)	(0.0000)	(0.0000)	(0.0000)	(0.0000)
q60	0.0113	0.0112	0.0115	0.0118	0.0143	**0.0185**	0.0244	**0.0304**	0.0330	**0.0371**
	(0.0000)	(0.0000)	(0.0000)	(0.0000)	(0.0000)	(0.0000)	(0.0000)	(0.0000)	(0.0000)	(0.0000)
q70	0.0135	0.0137	0.0137	0.0139	0.0170	**0.0216**	0.0289	**0.0345**	0.0388	**0.0380**
	(0.0000)	(0.0000)	(0.0000)	(0.0000)	(0.0000)	(0.0000)	(0.0000)	(0.0000)	(0.0000)	(0.0000)
q80	0.0126	0.0123	0.0121	0.0132	0.0172	**0.0220**	0.0264	**0.0314**	0.0332	**0.0366**
	(0.0000)	(0.0000)	(0.0000)	(0.0000)	(0.0000)	(0.0000)	(0.0000)	(0.0000)	(0.0000)	(0.0000)
q90	0.0108	0.0109	0.0112	0.0119	0.0155	**0.0195**	0.0244	**0.0272**	0.0266	**0.0284**
	(0.0000)	(0.0000)	(0.0000)	(0.0000)	(0.0000)	(0.0000)	(0.0000)	(0.0000)	(0.0000)	(0.0000)
q95	0.0111	0.0114	0.0121	0.0131	0.0163	**0.0188**	0.0215	**0.0241**	0.0229	**0.0246**
	(0.0000)	(0.0000)	(0.0000)	(0.0000)	(0.0000)	(0.0000)	(0.0000)	(0.0000)	(0.0000)	(0.0000)

Notes: OLS estimates and HAC $t_{\beta=0}$ p-values in brackets, from regression: $C_t = \alpha + \beta * t + u_t$.

Table 3
Arctic trend acceleration (CRU monthly station data)

names/periods	1900-2019, 1920-2019	1900-2019, 1910-2019	1900-2019, 1930-2019	1900-2019, 1940-2019	1900-2019, 1950-2019	1900-2019, 1960-2019	1900-2019, 1970-2019	1900-2019, 1980-2019	1900-2019, 1990-2019
mean	-0.0704	0.0304	-0.0128	-0.0260	**-0.0013**	0.0253	**0.0468**	0.0680	**0.0666**
	(0.9168)	(0.2241)	(0.7614)	(0.9498)	(0.5358)	(0.0055)	(0.0009)	(0.0000)	(0.0000)
iqr	0.0650	-0.0478	0.0022	0.0231	**0.0063**	-0.0094	**-0.0161**	-0.0276	**-0.0176**
	(0.0669)	(0.9705)	(0.4525)	(0.0542)	(0.3238)	(0.8112)	(0.8674)	(0.9374)	(0.7487)
q5	-0.4717	0.1615	-0.0396	-0.0656	**-0.0041**	0.0656	**0.1148**	0.1846	**0.1616**
	(1.0000)	(0.1142)	(0.7394)	(0.9310)	(0.5382)	(0.0207)	(0.0101)	(0.0000)	(0.0014)
q10	-0.2325	0.1954	0.0049	-0.0454	**0.0195**	0.0815	**0.1310**	0.1754	**0.1763**
	(0.9850)	(0.0448)	(0.4645)	(0.8296)	(0.3213)	(0.0027)	(0.0006)	(0.0000)	(0.0000)
q20	0.2229	0.0867	-0.0300	-0.0665	**-0.0304**	0.0247	**0.0673**	0.1130	**0.1227**
	(0.0000)	(0.1472)	(0.7780)	(0.9797)	(0.8562)	(0.0922)	(0.0063)	(0.0000)	(0.0000)
q30	-0.1777	0.0023	-0.0088	-0.0132	**0.0049**	0.0262	**0.0472**	0.0649	**0.0598**
	(1.0000)	(0.4802)	(0.6815)	(0.7968)	(0.3773)	(0.0139)	(0.0011)	(0.0000)	(0.0044)
q40	-0.1214	0.0210	-0.0029	-0.0157	**-0.0001**	0.0244	**0.0452**	0.0660	**0.0553**
	(0.9674)	(0.3329)	(0.5538)	(0.8108)	(0.5040)	(0.0205)	(0.0017)	(0.0000)	(0.0132)
q50	0.0385	0.0428	-0.0090	-0.0209	**-0.0051**	0.0206	**0.0397**	0.0562	**0.0573**
	(0.2998)	(0.0475)	(0.6866)	(0.9118)	(0.6655)	(0.0208)	(0.0022)	(0.0002)	(0.0024)
q60	0.0349	0.0097	0.0159	-0.0045	**0.0060**	0.0179	**0.0371**	0.0471	**0.0546**
	(0.2562)	(0.3863)	(0.1959)	(0.6234)	(0.2918)	(0.0390)	(0.0000)	(0.0000)	(0.0000)
q70	-0.0235	0.0120	-0.0004	0.0014	0.0076	0.0213	0.0368	0.0460	**0.0595**
	(0.7455)	(0.3030)	(0.5101)	(0.4383)	(0.1636)	(0.0036)	(0.0000)	(0.0000)	(0.0000)
q80	-0.0964	-0.0429	-0.0348	-0.0254	-0.0053	0.0101	0.0261	0.0353	**0.0374**
	(0.9512)	(0.9080)	(0.9681)	(0.9812)	(0.7017)	(0.1584)	(0.0050)	(0.0004)	(0.0019)
q90	-0.0327	-0.0520	-0.0334	-0.0426	**-0.0227**	-0.0107	**-0.0011**	0.0121	**-0.0002**
	(0.7445)	(0.9924)	(0.9803)	(0.9997)	(0.9868)	(0.8649)	(0.5357)	(0.1775)	(0.5044)
q95	-0.0597	-0.0627	-0.0419	-0.0383	**-0.0144**	-0.0023	**0.0044**	0.0128	**-0.0122**
	(0.8687)	(0.9999)	(0.9699)	(0.9947)	(0.8795)	(0.5928)	(0.3385)	(0.1815)	(0.8786)

Notes: For the acceleration hypothesis we run the system: $C_t = \alpha_1 + \beta_1 * t + u_t,\ t = 1, ..., s, ..., T, C_t = \alpha_2 + \beta_2 * t + u_t,\ t = s + 1, ..., T,$ and test the null hypothesis $\beta_2 = \beta_1$against the alternative $\beta_2 > \beta_1$. We show the value of the t-statistic and its HAC p-value in brackets.

Table 4
Globe trend acceleration (CRU monthly station data)

names/periods	1900-2019, 1920-2019	1900-2019, 1910-2019	1900-2019, 1930-2019	1900-2019, 1940-2019	1900-2019, 1950-2019	1900-2019, 1960-2019	1900-2019, 1970-2019	1900-2019, 1980-2019	1900-2019, 1990-2019
mean	0.0211	0.0110	0.0036	0.0030	**0.0097**	0.0180	**0.0249**	0.0270	**0.0267**
	(0.0719)	(0.0340)	(0.1788)	(0.2074)	(0.0034)	(0.0000)	(0.0000)	(0.0000)	(0.0000)
iqr	0.0383	0.0062	0.0039	-0.0054	**-0.0034**	0.0002	**0.0050**	0.0090	**0.0209**
	(0.1075)	(0.3838)	(0.3055)	(0.8125)	(0.7495)	(0.4856)	(0.1569)	(0.1378)	(0.0077)
q5	-0.0304	0.0327	0.0085	0.0099	**0.0167**	0.0241	**0.0279**	0.0247	**0.0058**
	(0.8762)	(0.0373)	(0.2009)	(0.1418)	(0.0216)	(0.0003)	(0.0064)	(0.0280)	(0.3432)
q10	-0.0376	-0.0137	-0.0036	0.0052	**0.0168**	0.0244	**0.0266**	0.0260	**0.0153**
	(0.9859)	(0.8657)	(0.6576)	(0.2805)	(0.0326)	(0.0001)	(0.0010)	(0.0054)	(0.0910)
q20	-0.0002	0.0060	0.0002	0.0072	**0.0152**	0.0229	**0.0267**	0.0280	**0.0227**
	(0.5055)	(0.3028)	(0.4861)	(0.0736)	(0.0019)	(0.0000)	(0.0000)	(0.0000)	(0.0037)
q30	0.0070	0.0118	0.0044	0.0064	**0.0094**	0.0157	**0.0213**	0.0197	**0.0167**
	(0.3305)	(0.0866)	(0.1680)	(0.0378)	(0.0051)	(0.0000)	(0.0000)	(0.0001)	(0.0061)
q40	0.0006	0.0144	0.0029	0.0016	**0.0048**	0.0134	**0.0228**	0.0264	**0.0294**
	(0.4869)	(0.0170)	(0.2514)	(0.3291)	(0.0776)	(0.0001)	(0.0000)	(0.0000)	(0.0000)
q50	0.0154	0.0042	0.0042	0.0001	**0.0046**	0.0140	**0.0231**	0.0269	**0.0289**
	(0.1528)	(0.2987)	(0.1679)	(0.4875)	(0.1273)	(0.0001)	(0.0000)	(0.0000)	(0.0000)
q60	0.0443	0.0094	0.0030	-0.0016	**0.0053**	0.0148	**0.0224**	0.0278	**0.0332**
	(0.0041)	(0.1384)	(0.2776)	(0.6298)	(0.1004)	(0.0000)	(0.0000)	(0.0000)	(0.0000)
q70	0.0479	0.0177	0.0068	0.0011	**0.0088**	0.0189	**0.0289**	0.0355	**0.0390**
	(0.0105)	(0.0160)	(0.1402)	(0.4203)	(0.0199)	(0.0000)	(0.0000)	(0.0000)	(0.0000)
q80	0.0499	0.0057	0.0007	-0.0045	**0.0033**	0.0133	**0.0219**	0.0271	**0.0361**
	(0.0393)	(0.3421)	(0.4652)	(0.7919)	(0.2053)	(0.0001)	(0.0000)	(0.0000)	(0.0000)
q90	0.0492	0.0012	-0.0022	-0.0036	**0.0064**	0.0150	**0.0232**	0.0261	**0.0324**
	(0.0076)	(0.4506)	(0.6513)	(0.7809)	(0.0746)	(0.0000)	(0.0000)	(0.0000)	(0.0000)
q95	0.0667	0.0163	0.0036	0.0034	**0.0090**	0.0141	**0.0190**	0.0195	**0.0211**
	(0.0000)	(0.0452)	(0.2910)	(0.2303)	(0.0058)	(0.0000)	(0.0000)	(0.0000)	(0.0000)

Notes: For the acceleration hypothesis we run the system: $C_t = \alpha_1 + \beta_1 * t + u_t,\ t = 1, ..., s, ..., T, C_t = \alpha_2 + \beta_2 * t + u_t,\ t = s + 1, ..., T,$ and test the null hypothesis $\beta_2 = \beta_1$against the alternative $\beta_2 > \beta_1$. We show the value of the t-statistic and its HAC p-value in brackets.

Table 5
Arctic external amplification (Arctic-Global)

periods/variables	1900-2019	1910-2019	1920-2019	1930-2019	1940-2019	1950-2019	1960-2019	1970-2019	1980-2019	1990-2019
mean	1.61	1.63	1.45	1.41	1.46	**1.53**	1.66	**1.65**	1.68	**1.79**
	(0.000)	(0.000)	(0.004)	(0.002)	(0.001)	(0.000)	(0.000)	(0.000)	(0.000)	(0.005)
iqr	-0.73	-0.77	-1.16	-1.34	-1.06	**-1.04**	-1.05	**-1.10**	-0.95	**-0.50**
	(1.000)	(1.000)	(1.000)	(1.000)	(1.000)	(1.000)	(1.000)	(1.000)	(1.000)	(0.933)
q05	3.34	2.99	1.86	2.21	1.74	**1.74**	1.88	**1.68**	1.11	**1.35**
	(0.000)	(0.000)	(0.012)	(0.006)	(0.017)	(0.001)	(0.000)	(0.012)	(0.381)	(0.284)
q10	3.42	3.30	2.21	2.00	2.20	**1.99**	2.01	**2.18**	1.74	**2.20**
	(0.000)	(0.000)	(0.001)	(0.015)	(0.000)	(0.000)	(0.000)	(0.000)	(0.027)	(0.028)
q20	2.49	2.66	2.42	2.26	2.18	**2.19**	2.30	**2.45**	2.42	**2.72**
	(0.000)	(0.000)	(0.000)	(0.000)	(0.000)	(0.000)	(0.000)	(0.000)	(0.001)	(0.022)
q30	1.74	1.81	1.97	2.12	2.28	**2.19**	2.39	**2.50**	2.71	**2.37**
	(0.000)	(0.000)	(0.001)	(0.000)	(0.000)	(0.000)	(0.000)	(0.000)	(0.001)	(0.070)
q40	1.56	1.70	1.70	1.49	1.87	**2.11**	2.32	**2.13**	2.40	**2.40**
	(0.003)	(0.000)	(0.000)	(0.004)	(0.000)	(0.000)	(0.000)	(0.001)	(0.001)	(0.010)
q50	1.49	1.56	1.30	1.32	1.36	**1.64**	1.92	**1.74**	1.92	**1.75**
	(0.004)	(0.002)	(0.024)	(0.009)	(0.010)	(0.001)	(0.000)	(0.002)	(0.000)	(0.001)
q60	1.10	1.16	1.13	1.23	1.14	**1.20**	1.36	**1.40**	1.46	**1.61**
	(0.241)	(0.128)	(0.179)	(0.026)	(0.110)	(0.067)	(0.005)	(0.009)	(0.014)	(0.001)
q70	0.98	1.07	1.08	1.13	1.08	**1.11**	1.20	**1.18**	1.21	**1.54**
	(0.559)	(0.345)	(0.328)	(0.099)	(0.258)	(0.161)	(0.043)	(0.070)	(0.101)	(0.000)
q80	1.05	0.95	0.96	0.96	1.02	**1.11**	1.19	**1.27**	1.37	**1.55**
	(0.321)	(0.655)	(0.604)	(0.631)	(0.450)	(0.175)	(0.064)	(0.009)	(0.008)	(0.000)
q90	0.76	0.66	0.54	0.47	0.57	**0.75**	0.87	**0.75**	1.03	**1.08**
	(0.951)	(0.992)	(0.998)	(1.000)	(1.000)	(1.000)	(0.943)	(0.921)	(0.392)	(0.352)
q95	0.64	0.49	0.38	0.51	0.69	**0.69**	0.82	**0.76**	0.99	**0.90**
	(0.984)	(0.995)	(1.000)	(1.000)	(0.994)	(0.991)	(0.890)	(0.893)	(0.548)	(0.676)

Notes: OLS estimates and HAC p-values (in brackets), of the t-statistic of testing $H_0 : \beta_1 = 1$ versus $H_a : \beta_1 > 1$ in the regression: $C_t = \beta_0 + \beta_1 * mean_t + \epsilon_t$. *mean* refers to the average of the Globe temperature distribution and C_t to the different characteristics of the Arctic temperature distribution.

Table 6
Arctic local amplification (Arctic-Arctic)

periods/variables	1900-2019	1910-2019	1920-2019	1930-2019	1940-2019	1950-2019	1960-2019	1970-2019	1980-2019	1990-2019
iqr	-0.45	-0.49	-0.83	-1.16	-0.96	-0.72	-0.68	-0.70	-0.67	-0.61
	(1.000)	(1.000)	(1.000)	(1.000)	(1.000)	(1.000)	(1.000)	(1.000)	(1.000)	(1.000)
q05	2.30	2.10	1.56	1.37	1.26	1.18	1.22	1.11	0.93	1.15
	(0.000)	(0.000)	(0.000)	(0.040)	(0.029)	(0.008)	(0.005)	(0.113)	(0.785)	(0.113)
q10	2.31	2.15	1.73	1.38	1.51	1.36	1.31	1.42	1.32	1.60
	(0.000)	(0.000)	(0.000)	(0.015)	(0.000)	(0.000)	(0.000)	(0.000)	(0.003)	(0.000)
q20	1.55	1.70	1.68	1.78	1.52	1.44	1.40	1.49	1.50	1.64
	(0.000)	(0.000)	(0.000)	(0.000)	(0.000)	(0.000)	(0.000)	(0.000)	(0.000)	(0.000)
q30	0.99	1.04	1.30	1.60	1.70	1.48	1.44	1.53	1.61	1.43
	(0.562)	(0.206)	(0.000)	(0.000)	(0.000)	(0.000)	(0.000)	(0.000)	(0.000)	(0.004)
q40	0.96	0.97	1.11	1.13	1.34	1.43	1.44	1.34	1.44	1.35
	(0.741)	(0.651)	(0.044)	(0.019)	(0.000)	(0.000)	(0.000)	(0.000)	(0.000)	(0.013)
q50	0.82	0.84	0.83	0.93	0.95	1.07	1.11	1.04	1.06	0.95
	(0.998)	(0.990)	(0.996)	(0.867)	(0.798)	(0.158)	(0.068)	(0.310)	(0.245)	(0.658)
q60	0.64	0.65	0.68	0.78	0.71	0.77	0.79	0.83	0.82	0.80
	(1.000)	(1.000)	(1.000)	(1.000)	(1.000)	(1.000)	(1.000)	(0.998)	(0.996)	(0.985)
q70	0.53	0.60	0.63	0.69	0.67	0.67	0.70	0.70	0.71	0.77
	(1.000)	(1.000)	(1.000)	(1.000)	(1.000)	(1.000)	(1.000)	(1.000)	(1.000)	(0.998)
q80	0.59	0.54	0.63	0.65	0.64	0.68	0.68	0.73	0.73	0.72
	(1.000)	(1.000)	(1.000)	(1.000)	(1.000)	(1.000)	(1.000)	(1.000)	(1.000)	(0.998)
q90	0.52	0.49	0.50	0.38	0.35	0.42	0.45	0.40	0.46	0.34
	(1.000)	(1.000)	(1.000)	(1.000)	(1.000)	(1.000)	(1.000)	(1.000)	(1.000)	(1.000)
q95	0.46	0.38	0.44	0.47	0.42	0.42	0.43	0.37	0.40	0.26
	(1.000)	(1.000)	(1.000)	(1.000)	(1.000)	(1.000)	(1.000)	(1.000)	(1.000)	(1.000)

Notes: OLS estimates and HAC p-values (in brackets), of the t-statistic of testing $H_0 : \beta_1 = 1$ versus $H_a : \beta_1 > 1$ in the regression: $C_t = \beta_0 + \beta_1 * mean_t + \epsilon_t$. *mean* refers to the average of the Arctic temperature distribution and C_t to the different characteristics of the Arctic temperature distribution.

Table 7
Global amplification (Global-Global)

periods/variables	1900-2019	1910-2019	1920-2019	1930-2019	1940-2019	1950-2019	1960-2019	1970-2019	1980-2019	1990-2019
iqr	-0.01	-0.07	-0.14	-0.25	-0.32	-0.31	-0.28	-0.20	-0.34	-0.24
	(1.000)	(1.000)	(1.000)	(1.000)	(1.000)	(1.000)	(1.000)	(1.000)	(1.000)	(1.000)
q05	1.66	1.75	1.78	2.06	2.07	1.89	1.70	1.49	1.37	1.08
	(0.000)	(0.000)	(0.000)	(0.000)	(0.000)	(0.000)	(0.001)	(0.002)	(0.070)	(0.412)
q10	1.39	1.45	1.59	1.73	1.90	1.82	1.69	1.63	1.60	1.44
	(0.000)	(0.000)	(0.000)	(0.000)	(0.000)	(0.000)	(0.000)	(0.000)	(0.000)	(0.000)
q20	1.11	1.16	1.21	1.24	1.28	1.25	1.27	1.19	1.38	1.43
	(0.029)	(0.010)	(0.002)	(0.001)	(0.000)	(0.001)	(0.005)	(0.062)	(0.001)	(0.017)
q30	0.91	0.91	0.95	0.98	1.00	1.02	1.00	0.99	1.09	1.03
	(0.974)	(0.972)	(0.828)	(0.661)	(0.540)	(0.356)	(0.520)	(0.560)	(0.104)	(0.405)
q40	0.81	0.80	0.75	0.76	0.75	0.79	0.80	0.89	0.87	0.88
	(1.000)	(1.000)	(1.000)	(1.000)	(1.000)	(1.000)	(1.000)	(0.984)	(0.951)	(0.847)
q50	0.83	0.81	0.78	0.72	0.71	0.75	0.78	0.81	0.86	0.88
	(1.000)	(1.000)	(1.000)	(1.000)	(1.000)	(1.000)	(1.000)	(1.000)	(0.998)	(0.933)
q60	0.86	0.84	0.82	0.74	0.70	0.73	0.79	0.86	0.84	0.95
	(0.998)	(0.999)	(1.000)	(1.000)	(1.000)	(1.000)	(1.000)	(0.999)	(0.999)	(0.793)
q70	1.01	1.00	0.95	0.86	0.80	0.84	0.93	0.97	1.00	0.97
	(0.405)	(0.476)	(0.797)	(0.994)	(1.000)	(1.000)	(0.906)	(0.706)	(0.529)	(0.604)
q80	0.93	0.89	0.85	0.83	0.82	0.85	0.86	0.86	0.84	0.90
	(0.887)	(0.983)	(0.997)	(0.999)	(1.000)	(0.999)	(0.999)	(0.994)	(0.995)	(0.801)
q90	0.81	0.78	0.77	0.73	0.73	0.74	0.76	0.74	0.65	0.70
	(1.000)	(1.000)	(1.000)	(1.000)	(1.000)	(1.000)	(1.000)	(1.000)	(1.000)	(1.000)
q95	0.74	0.73	0.71	0.68	0.70	0.65	0.63	0.63	0.56	0.58
	(1.000)	(1.000)	(1.000)	(1.000)	(1.000)	(1.000)	(1.000)	(1.000)	(1.000)	(1.000)

Notes: OLS estimates and HAC p-values (in brackets), of the t-statistic of testing $H_0 : \beta_1 = 1$ versus $H_a : \beta_1 > 1$ in the regression: $C_t = \beta_0 + \beta_1 * mean_t + \epsilon_t$. *mean* refers to the average of the Globe temperature distribution and C_t to the different characteristics of the Global temperature distribution.

Table 8
OLS slope linear trend estimates (CRU monthly station data, Antarctic, 1960-2022)

	Trend test by periods	
names/periods	1960-2022	1990-2022
mean	0.0025	0.0111
	(0.4554)	(0.2227)
iqr	0.0110	0.0186
	(0.3061)	(0.2646)
q05	-0.0001	0.0520
	(0.9931)	(0.0233)
q10	0.0126	-0.0051
	(0.0960)	(0.8862)
q20	-0.0043	0.0159
	(0.6813)	(0.3623)
q30	0.0069	0.0022
	(0.3592)	(0.8992)
q40	0.0010	0.0125
	(0.8970)	(0.4587)
q50	0.0007	0.0017
	(0.9168)	(0.9077)
q60	0.0039	0.0122
	(0.5857)	(0.3691)
q70	0.0052	0.0136
	(0.3181)	(0.1160)
q80	0.0057	0.0024
	(0.1453)	(0.7794)
q90	0.0074	0.0092
	(0.0308)	(0.2812)
q95	-0.0011	-0.0053
	(0.8486)	(0.5603)

Notes: OLS estimates and HAC $t_{\beta=0}$ p-values in brackets, from regression: $C_t = \alpha + \beta * t + u_t$.

6 Figures

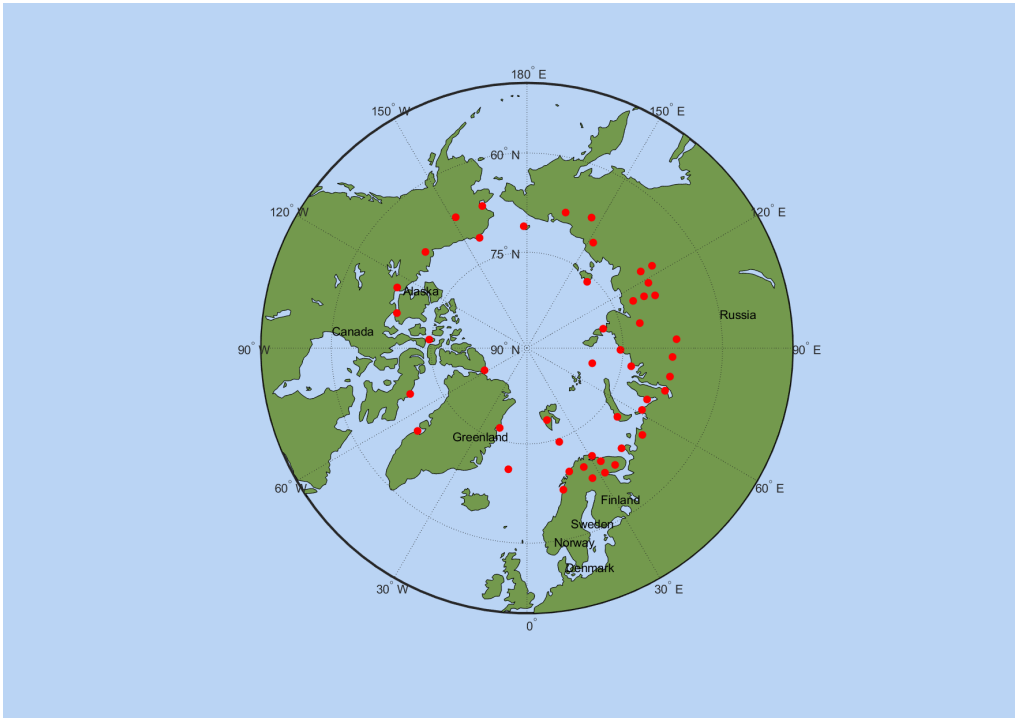

Notes: Stations have been selected from month-station units that provide data for the whole sample 1950-2019. The total number is 48.

Figure 1
Geographical coordinates of selected stations in the Arctic polar circle (CRU data)

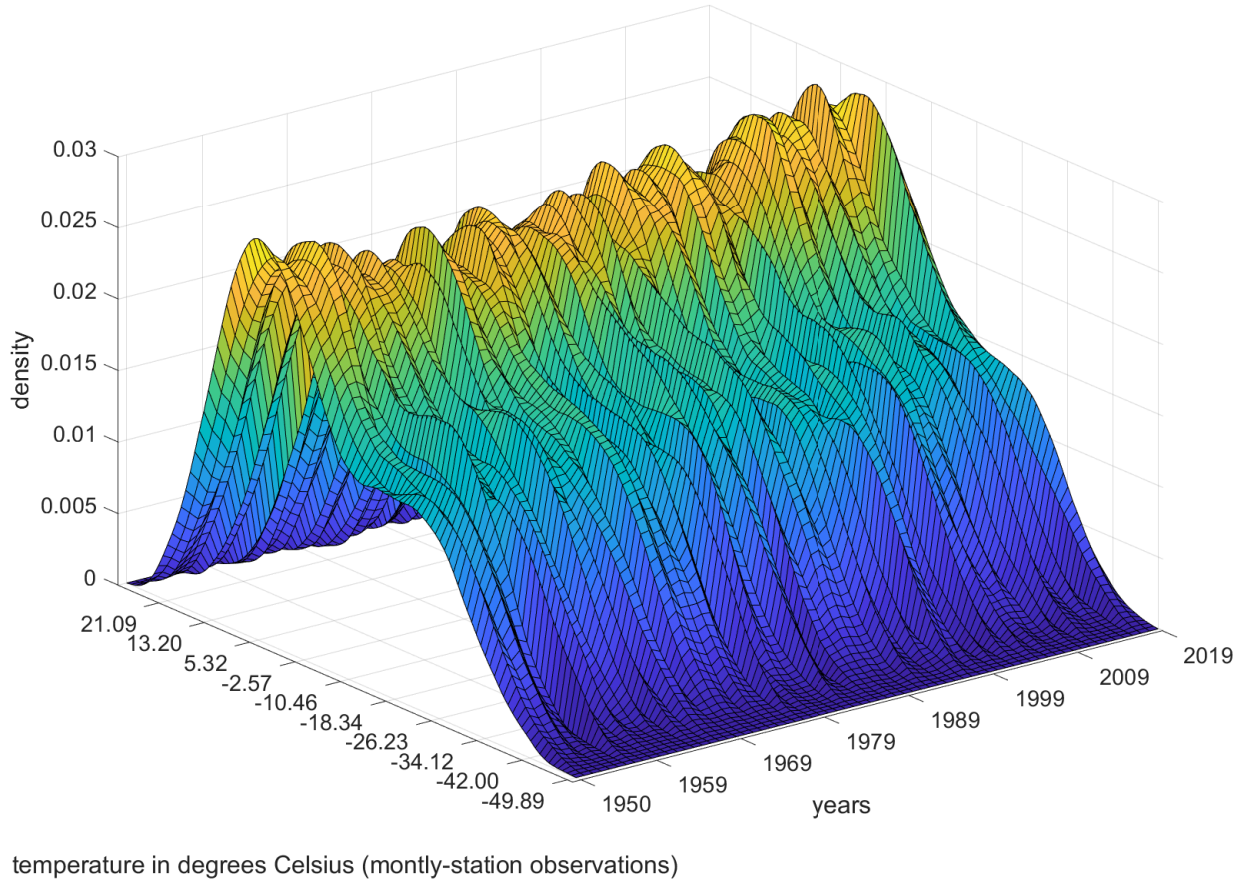

Notes: Stations have been selected from month-station units that provide data for the whole sample in the period 1950-2019. The total number is 408.

Figure 2
Density of selected month-station units (Arctic Polar Circle CRU data)

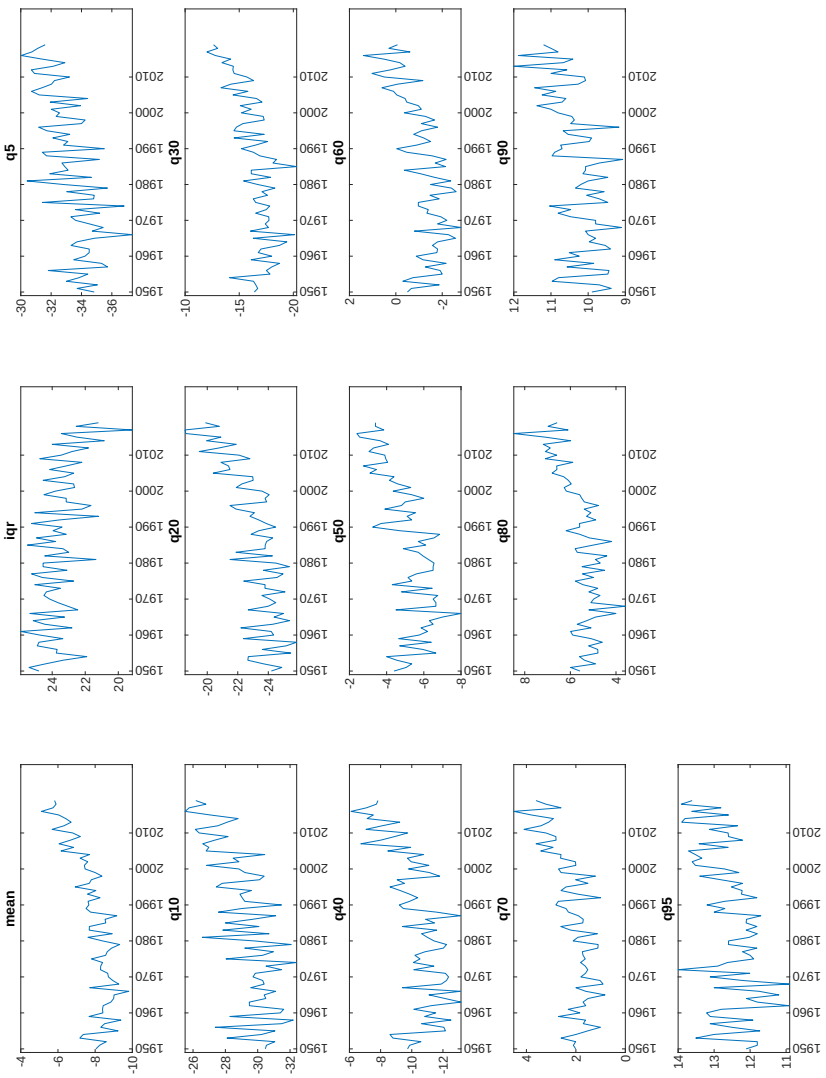

Notes: Characteristics are calculated from month-station units that provide data for the whole sample in the period 1950-2019. The total number of units is 408. Temperatures are in degree Celsius.

Figure 3
Temperature characteristics of the Arctic polar circle (CRU data)

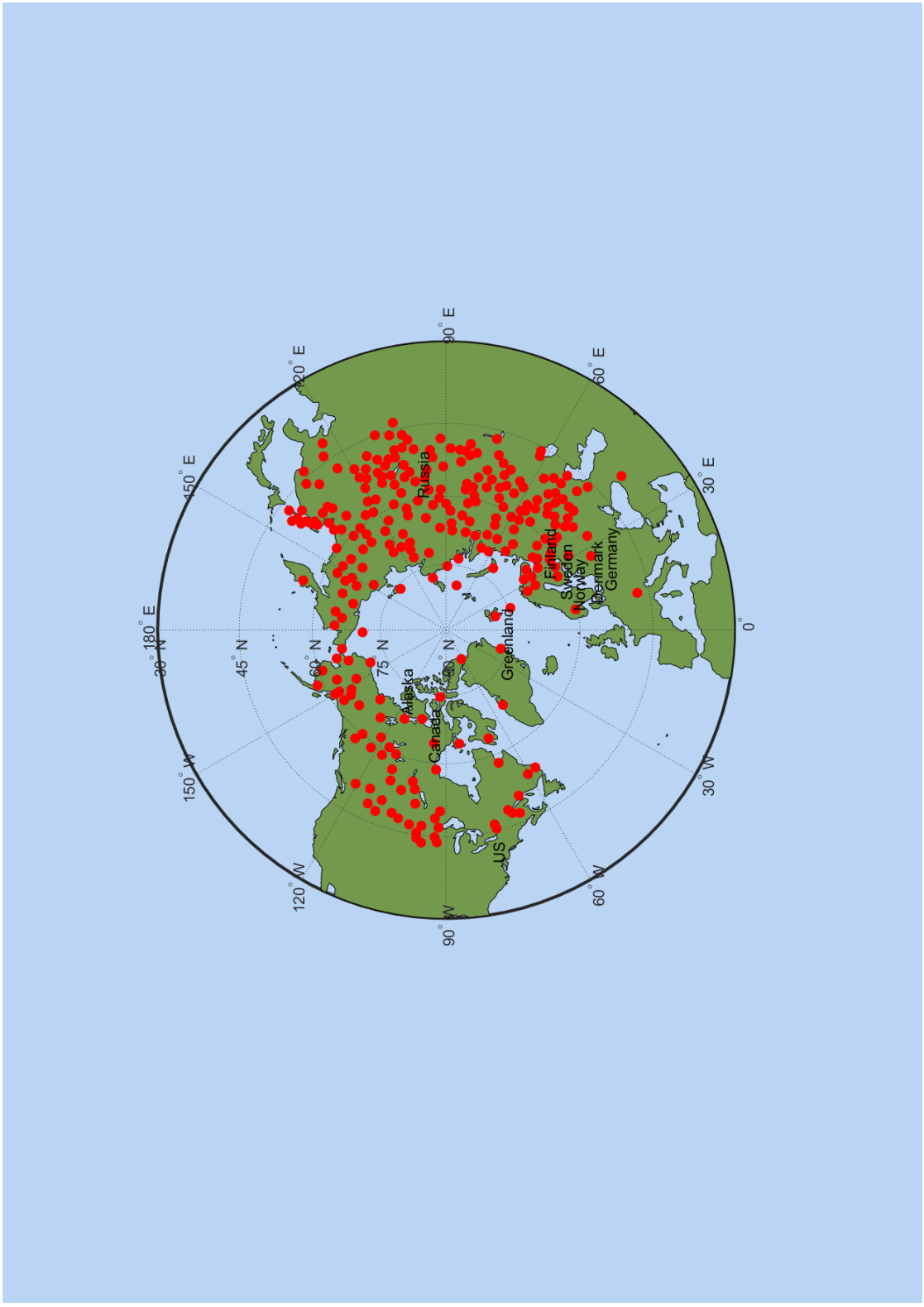

Notes: Stations have been selected from month-station units that provide data for the whole sample 1950-2019 and are situated in the *q05* quantile. Four stations in the Antarctic Polar Circle have been removed. The total number is 272.

Figure 4
Geographical coordinates of global stations in the *q05* quantile (CRU data)

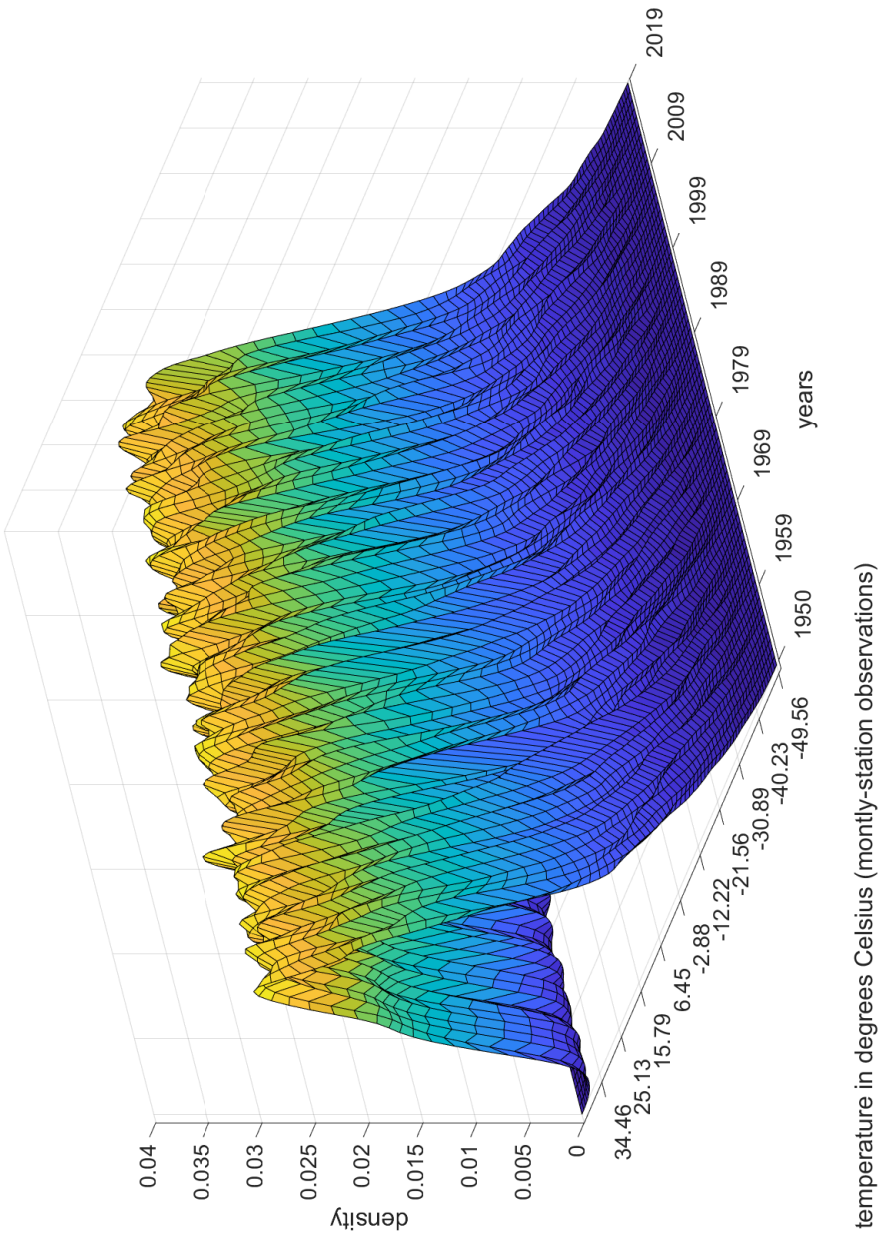

Figure 5
Density of selected month-station units (Global CRU data)

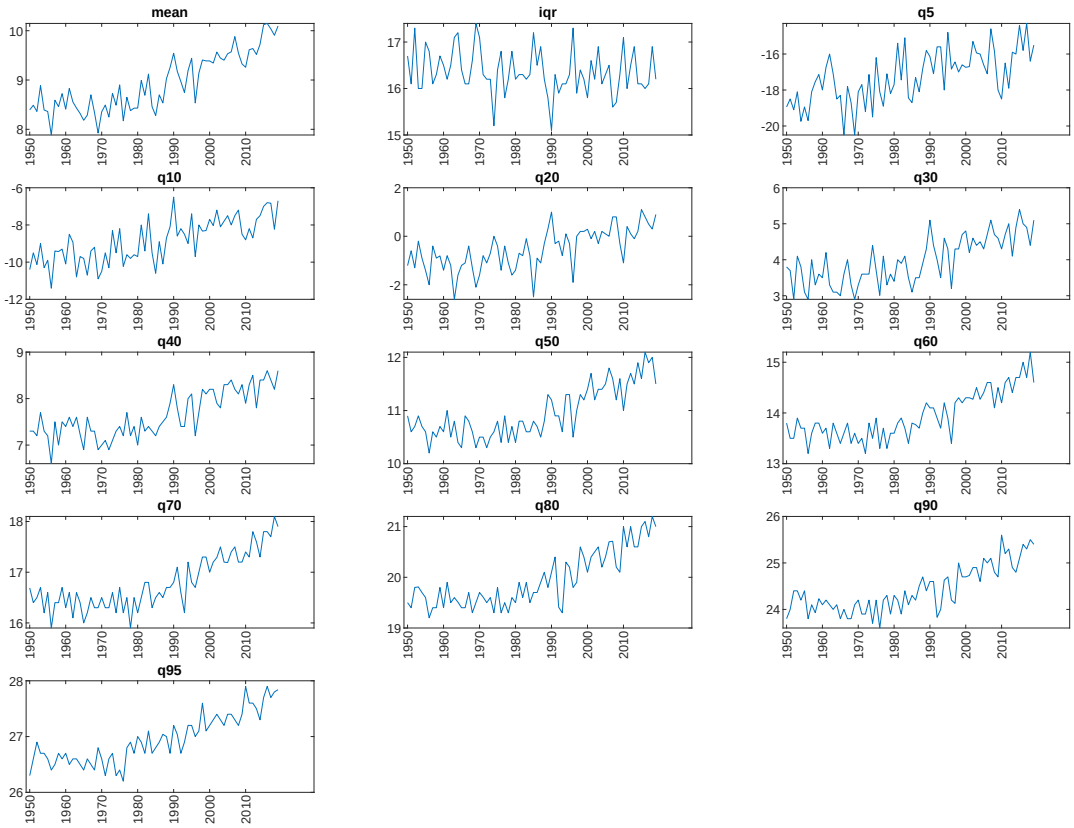

Notes: Characteristics are calculated from month-station units that provide data for the whole sample in the period 1950-2019. The total number of units is 9402. Temperatures are in degree Celsius.

Figure 6
Temperature characteristics of the Global temperatures (CRU data)

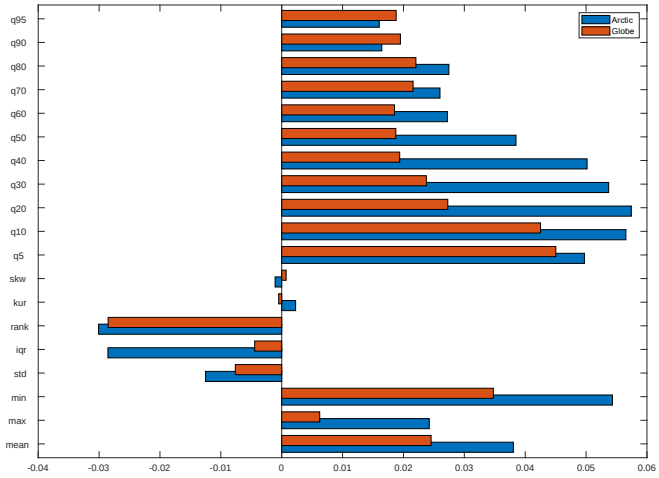

Notes: Characteristics are calculated from month-station units that provide data for the whole sample in the period 1950-2019. The X axis shows the slope coefficients representing degrees Celsius per year.

Figure 7
Globe and Arctic trend slope comparison (CRU Global and Arctic Polar Circle stations)

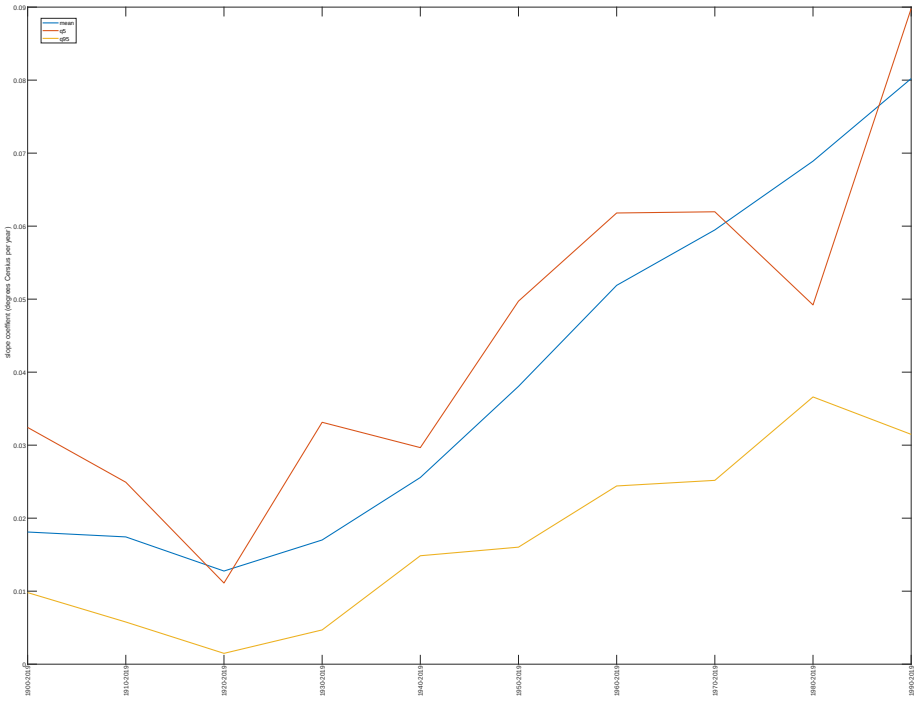

Notes: Characteristics are calculated from month-station units that provide data for the whole sample in the period 1950-2019. The total number of units is 408.

Figure 8
Evolution of trend slopes of selected quantiles in the Arctic polar circle (CRU data)

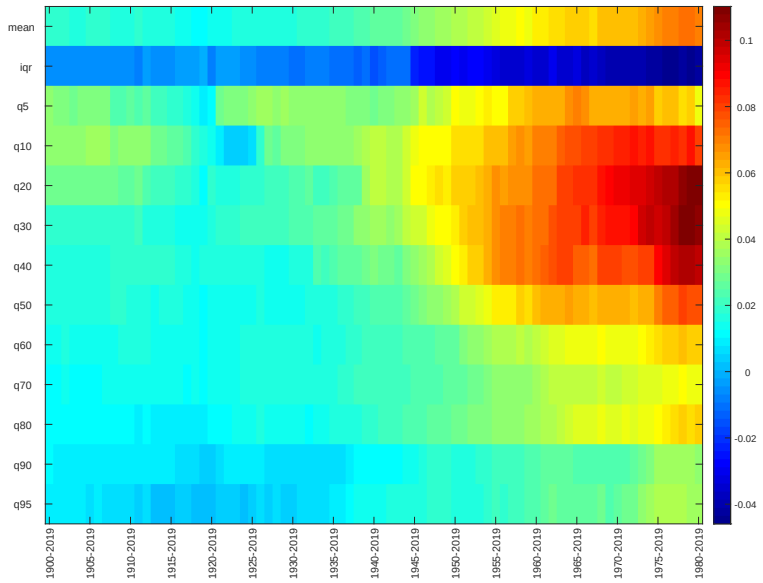

Notes: Y axis: trend coefficients of the different quantiles. X axis time intervals from 1900-1950,1900-1951,...,1900-2019. The scale of colors represents sign and intensity.

Figure 9
Evolution of the trend slopes of temperature characteristics of the Arctic

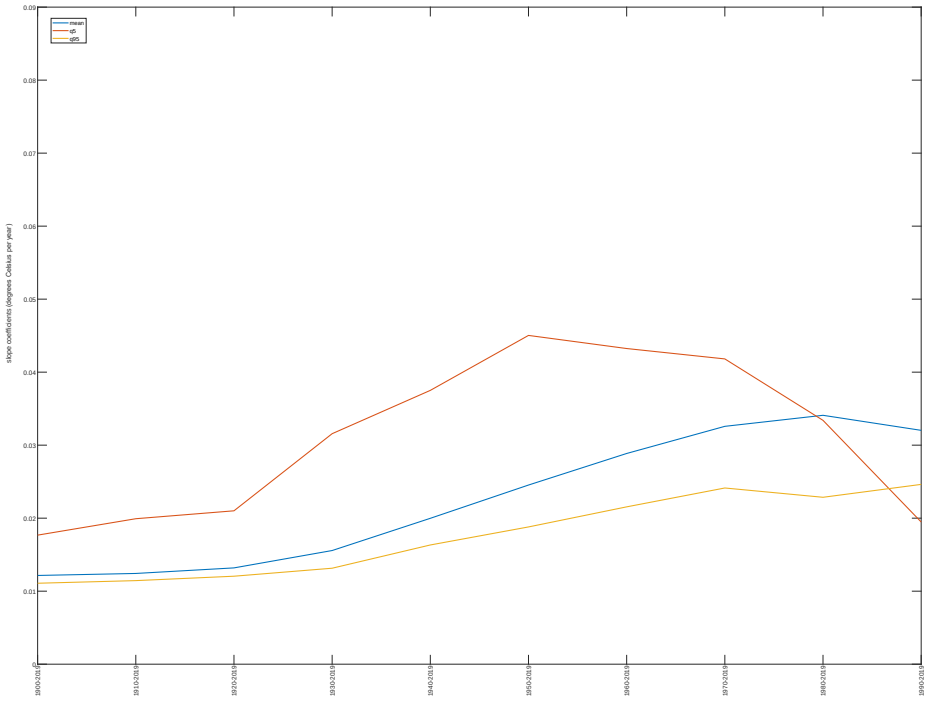

Notes: Characteristics are calculated from month-station units that provide data for the whole sample in the period 1950-2019.

Figure 10
Evolution trend slopes of selected quantiles by periods of the Globe

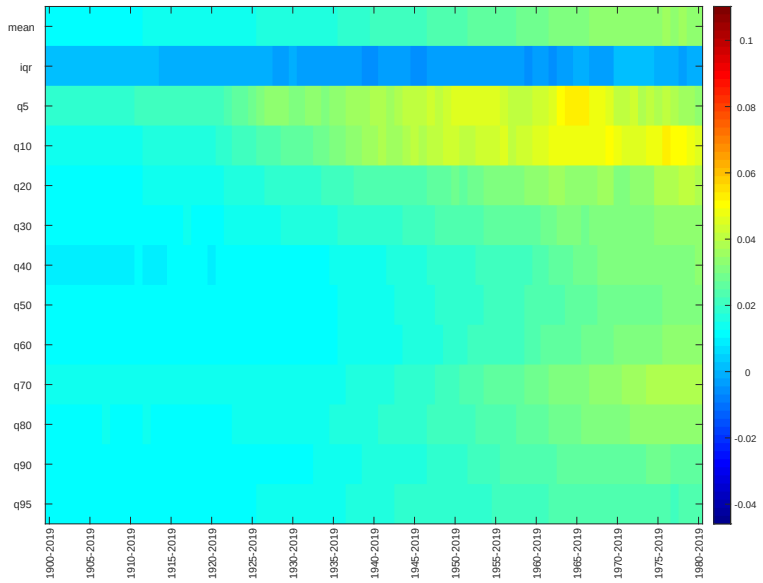

Notes: Y axis: trend coefficients of the different quantiles. X axis time intervals from 1900-1950,1900-1951,...,1900-2019. The scale of colors represents sign and intensity.

Figure 11
Evolution of the trend slopes of temperature characteristics of the Globe

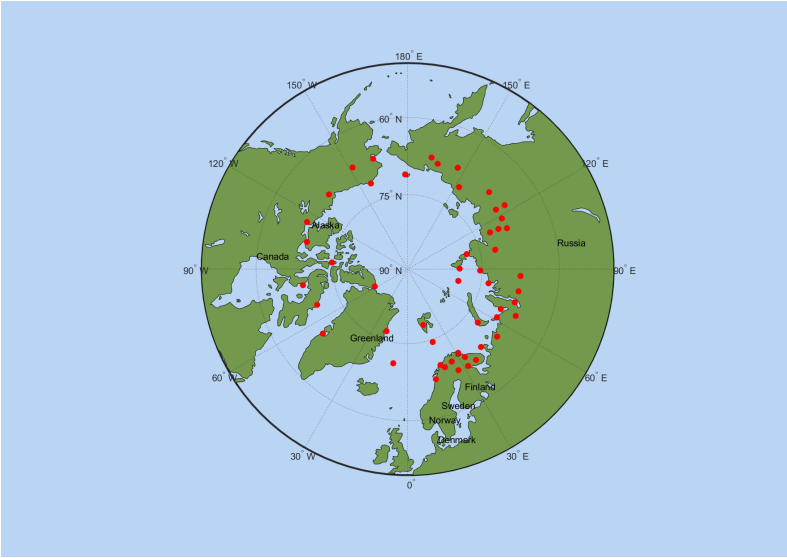

(a) Arctic

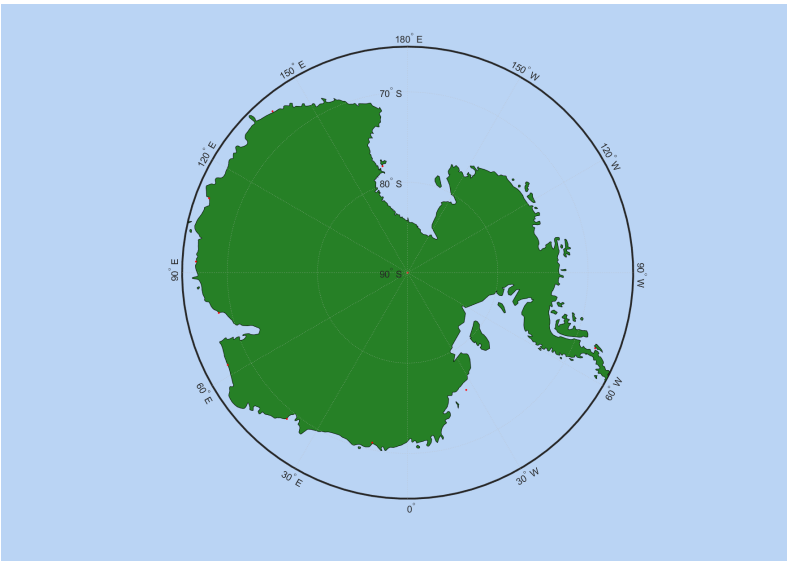

(b) Antarctic

Notes: Stations have been selected from month-station units of Arctic and Antarctic polar circle (latitude hither than 60^{o}N and lower than -60^{o}S) that provide data for the whole sample 1960-2019. The total number is 477 and 114, respectively.

Figure 12
Selected stations in both poles (1960-2022)

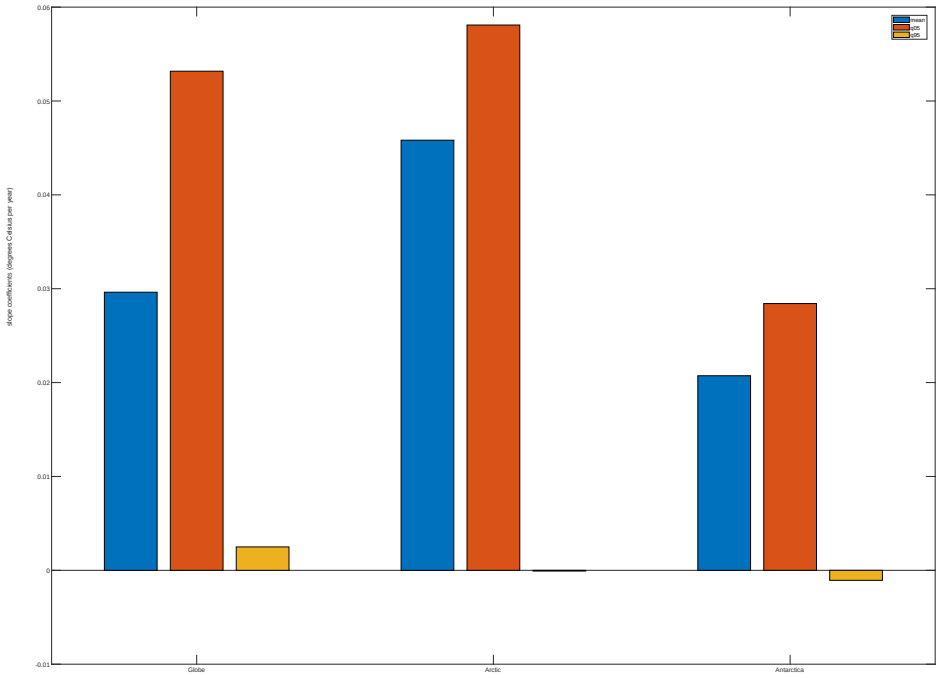

Notes: Stations have been selected from month-station units of Arctic and Antarctic polar circle (latitude hither than 60°N and lower than -60°S) that provide data for the whole sample 1960-2019. The total number is 477 and 114, respectively. The total number of units for the Globe is 9402.

Figure 13
Comparing slope trend coefficients (1960-2022)

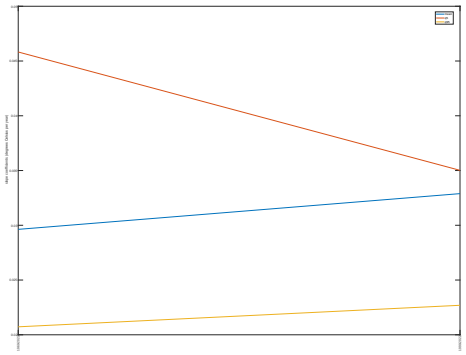

(a) Globe

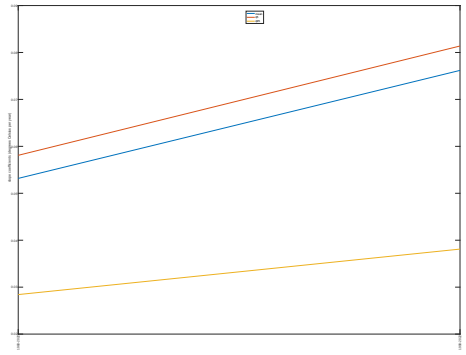

(b) Arctic

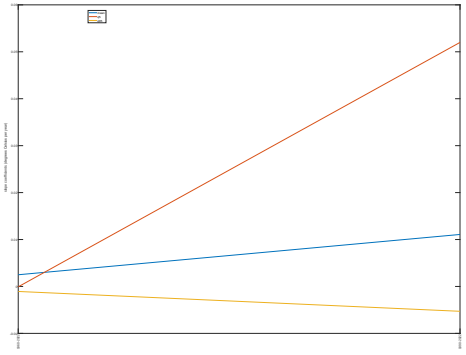

(c) Antarctic

Figure 14
Evolution of trend slope for selected quantiles

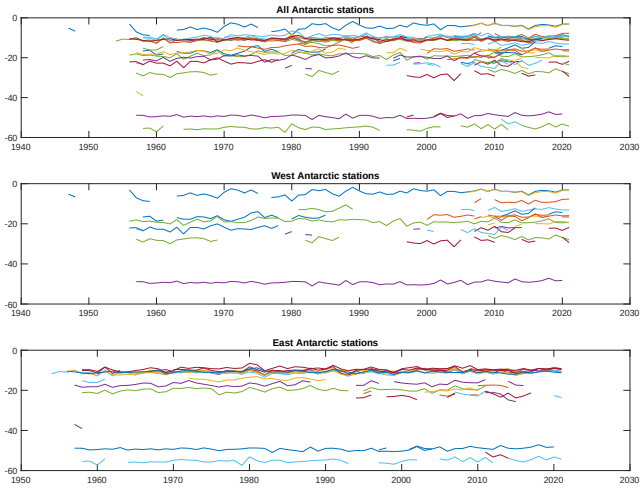

(a) Stations

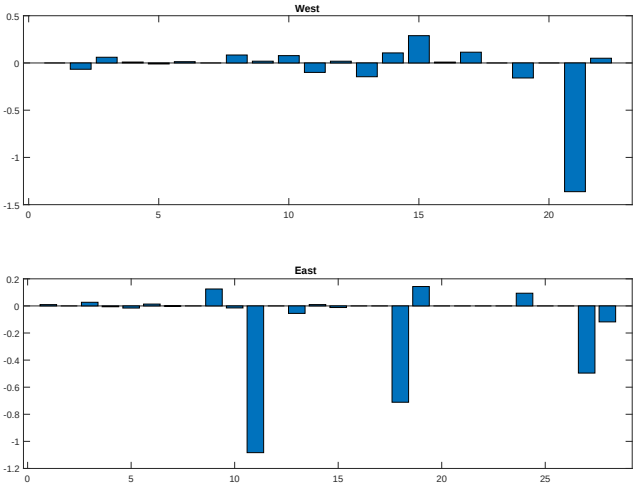

(b) Temperature Increase

Figure 15
Analysis of the Antarctic

7 Appendix

7.1 Additional results

Table A1
Unit root tests (Arctic)

Characteristic	ADF-SBIC	p-value	lags
mean	-2.80	0.204	4
iqr	-9.62	0.000	0
q05	-9.41	0.000	0
q10	-8.65	0.000	0
q20	-6.38	0.000	0
q30	-3.15	0.104	4
q40	-5.72	0.000	0
q50	-5.62	0.000	0
q60	-5.77	0.000	0
q70	-5.45	0.000	0
q80	-3.92	0.017	1
q90	-7.03	0.000	0
q95	-6.87	0.000	0

Notes: Dickey-Fuller (1979) unit root tests. Lag selection according to Schwarz Bayesian criteria (SBIC).

Table A2
Unit root tests (Antarctic)

Characteristic	ADF-SBIC	p-value	lags
mean	-6.75	0.000	0
iqr	-8.47	0.000	0
q05	-8.84	0.000	0
q10	-8.35	0.000	0
q20	-7.79	0.000	0
q30	-5.02	0.000	1
q40	-7.52	0.000	0
q50	-7.33	0.000	0
q60	-6.59	0.000	0
q70	-4.84	0.002	3
q80	-7.47	0.000	0
q90	-8.03	0.000	0
q95	-5.88	0.000	0

Notes: Dickey-Fuller (1979) unit root tests. Lag selection according to Schwarz Bayesian criteria (SBIC).

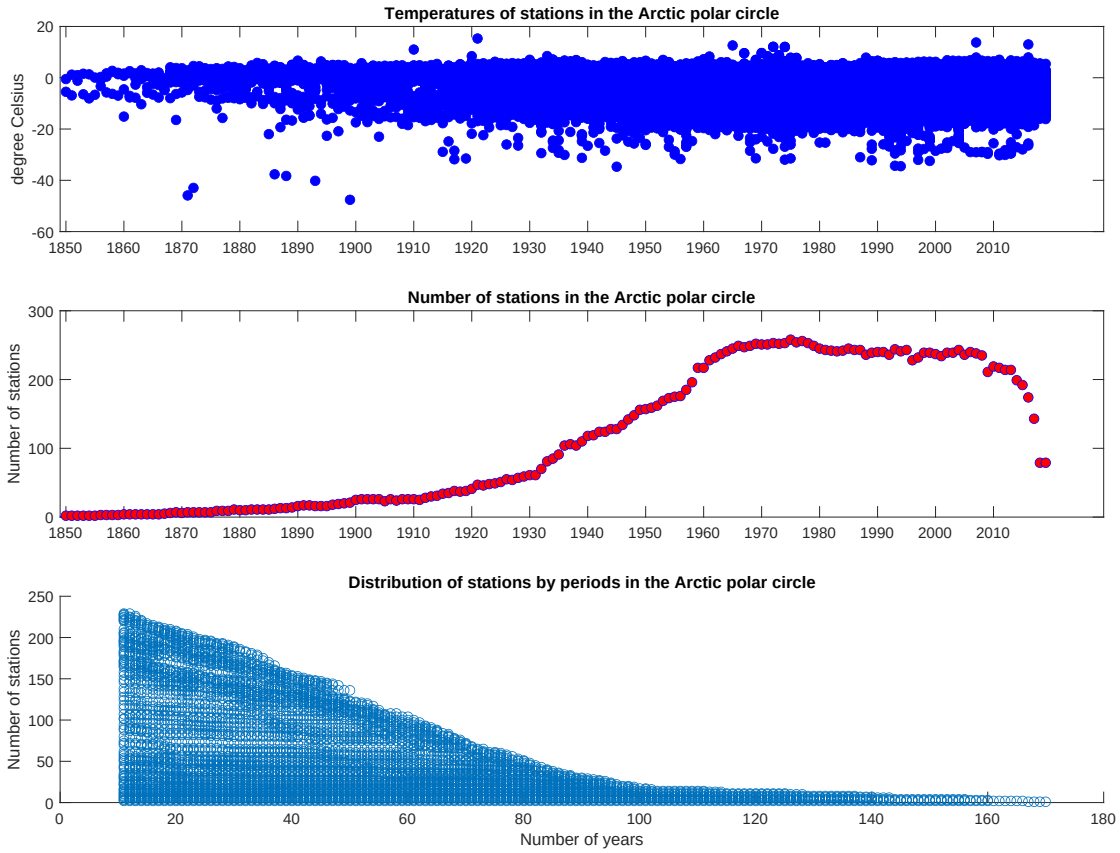

Notes: Stations have been selected from month-station units of Arctic polar circle (latitude hither than 66.5^{o}N) that provide data for the whole sample 1850-2019. The total number is 340.

Figure A1

Selection process of stations and time period of the Arctic polar circle (CRU data)

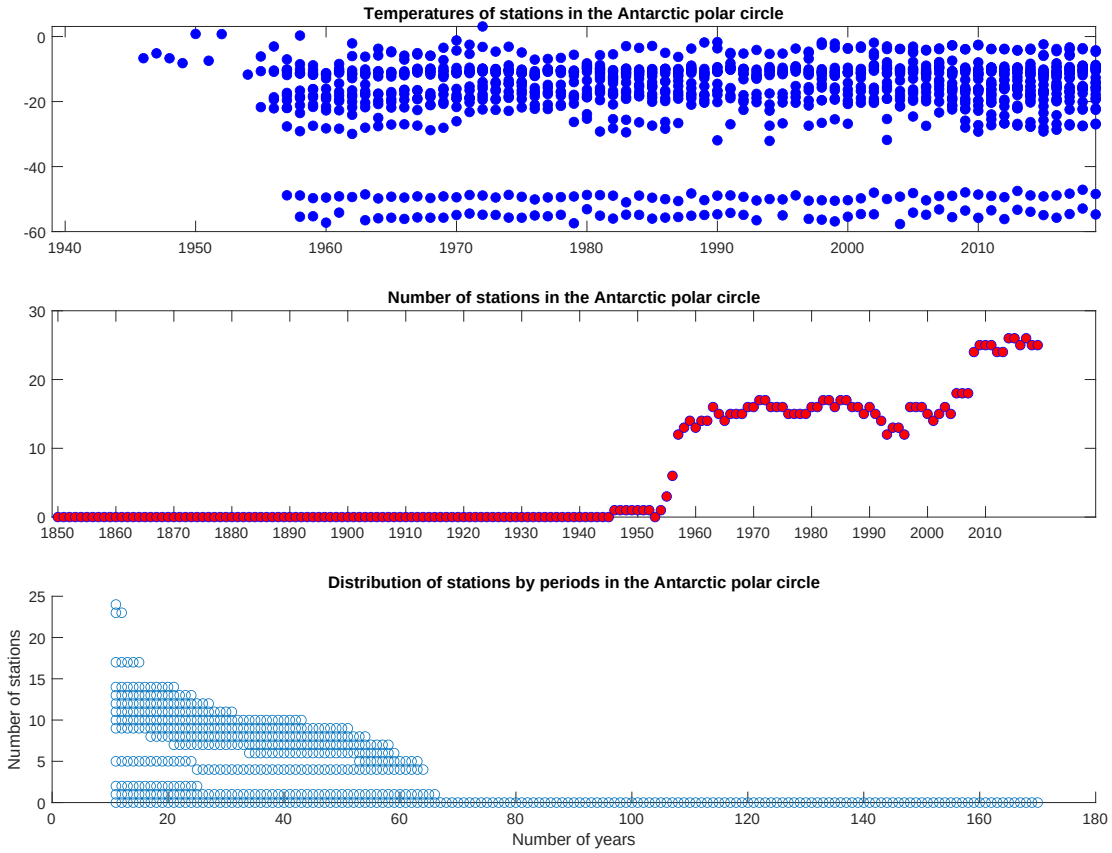

Notes: Stations have been selected from month-station units of Antarctic polar circle (latitude lower than -66.5^{o}S) that provide data for the whole sample 1850-2019. The total number is 32.

Figure A2

Selection process of stations and time period of the Antarctic polar circle (CRU data)

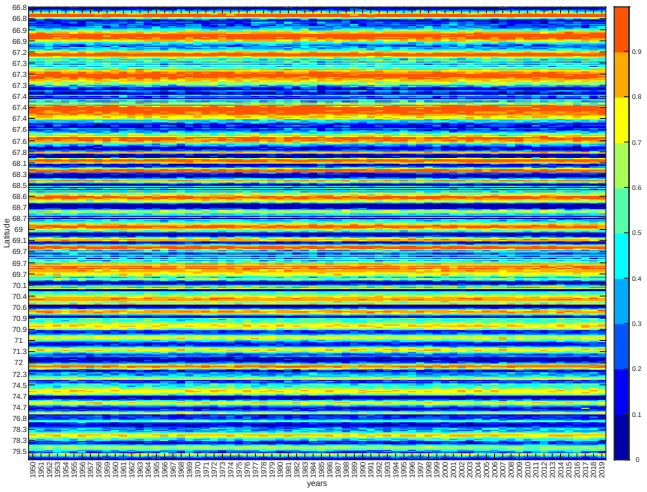

(a) By scale

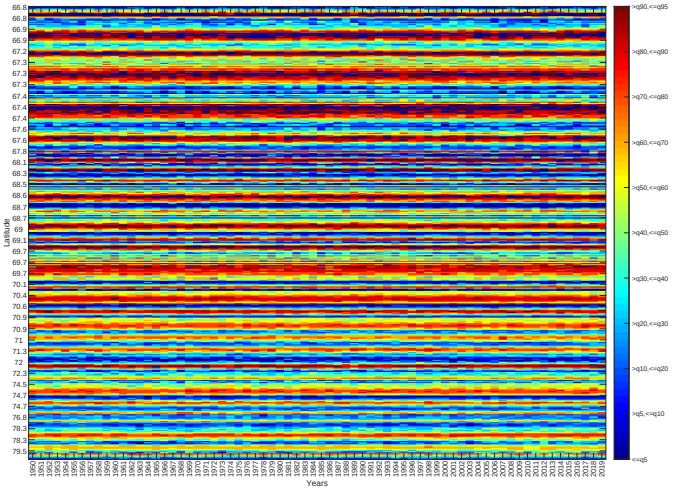

(b) By quantiles

Figure A3
Evolution of the position of the stations by quantiles and time

7.2 Two asymptotically equivalent methods to calculate Arctic Amplification, AA_t

Let's assume:

$$P_t = \alpha_p + \beta_p t + \epsilon_t \tag{7}$$

and

$$G_t = \alpha_G + \beta_G t + \varepsilon_t \tag{8}$$

where P_t=temperature in the Arctic at time "t"; G_t=temperature in the Globe at time "t"; t=1,2,3,...is a deterministic trend; ϵ_t and ε_t are I(0) processes (see footnote...).

1. Rantannen et al. (2022)

$$AA_t = \frac{\Delta P_t}{\Delta G_t} = \frac{\beta_p}{\beta_G} \tag{9}$$

   It can be estimated by $\frac{\widehat{\beta_p}}{\widehat{\beta_G}}$ but it is no easy to construct confidence intervals.

2. Our way

$$P_t = \alpha + \beta G_t + \xi_t \tag{10}$$

   $AA_t = \widehat{\beta}$ easy to test and construct confidence intervals.

The equivalence (asymptotically):

$$\alpha_p + \beta_p t + \epsilon_t = \alpha + \beta(\alpha_G + \beta_G t) + \varepsilon_t \tag{11}$$

dividing by t and making $t \to \infty$

$$\underbrace{\frac{\alpha_p}{t}}_{\longrightarrow 0} + \beta_p + \underbrace{\frac{\epsilon_t}{t}}_{\longrightarrow 0} = \underbrace{\frac{\alpha}{t}}_{\longrightarrow 0} + \underbrace{\frac{\beta\alpha_G}{t}}_{\longrightarrow 0} + \beta\beta_G + \underbrace{\frac{\varepsilon_t}{t}}_{\longrightarrow 0} \tag{12}$$

$$\beta = \frac{\beta_p}{\beta_G} \tag{13}$$

This method has the advantage of being able to estimate AA_t directly from a regression, where other control variables could be included. Testing significance and constructing confidence intervals is straightforward, while in the method of Rantannen et al. (2022) one would have to resort to bootstrap methods designed specifically for the case.